A comprehensive review of enhanced heat transfer with ribs/baffles in channels

Smith Eiamsa-ard[1],*, Arnut Phila[1], Khwanchit Wongcharee[1], Naoki Maruyama[2,3] and Masafumi Hirota[4]

[1]Department of Mechanical Engineering, Mahanakorn University of Technology, Bangkok, 10530, Thailand

[2]Division of Mechanical Engineering, Graduate School of Engineering, Mie University, Tsu, Mie, 514-8507, Japan

[3]Engineering Innovation Unit, Graduate School of Regional Innovation Studies, Mie University, Tsu, Mie, 514-8507, Japan

[4]Department of Mechanical Engineering, Faculty of Engineering, Aichi Institute of Technology, Toyota, Aichi, 470-0392, Japan

*ผู้ประพันธ์บรรณกิจ smith@mut.ac.th

ABSTRACT

The paper discusses the evolution and current state of heat transfer augmentation technologies utilized in various thermal energy systems, such as solar air heaters, solar thermal systems, and gas turbines. Several turbulence generators, instance ribs and baffles, are regarded an efficient methods of increasing heat transfer rate to moving air in the ducts of solar air heaters, heat exchangers, and for turbine blade cooling. The application of rib/baffles is an excellent method for enhancing heat transfer rate to a flowing fluid inside the channel/duct of a solar air heater and in turbine blade cooling. This paper seeks to present an in-depth assessment of research activity in increased heat transfer in its presentation of ribs/baffles in channels. It gives readers a thorough understanding of the principles of enhanced heat transfer with ribs and baffles, how this knowledge has evolved over time. The effects of a variety of rib/baffle shapes on the heat transfer rate and pressure loss behaviors of solar air heaters are been addressed. The most effective ribs/baffles for augmenting heat transfer and minimizing pressure drop are those that have been carefully engineered to enhance the thermal performance factor. The mechanics of heat transfer enhancement and flow structure around the ribs/baffles will be the main topics of this review. We have done a thorough investigation into the heat transfer mechanism in a channel with different rib and baffles turbulators before drawing our conclusions from the literature review.

Keywords: Baffle, channel, enhanced heat transfer, rib, rough surface, thermal performance, turbulator

1. Introduction

Reduced global resources and environmental considerations have necessitated the development of more efficient heat-transfer device with higher heat transfer rates. Engineers responsible for the design and operation of such systems must now prioritize both the reduction of energy lost due to inefficient use and the enhancement of energy transfer in the form of heat in light of the global increase in energy demand. Improvements in heat transfer have been suggested using a variety of methods. The methods may be split down into two categories: those that do not need any external power sources, known as "passive," and those that do, known as "active," which do require such sources.

The major technique of passive heat transfer enhancement is modifying heat transfer surfaces through different forms/designs. The viable approaches include installing baffles, ribs, fins and blocks, or forming grooves, dimpled and rough surfaces. Heat-transfer enhancement is achieved increased surface area (surface extension) and also by increasing turbulence (mixing). Modified surfaces are used in numerous equipment including heat exchangers, solar air heaters, nuclear reactor fuel elements, turbine blades, electronic boards and various components, among others. Improved heat-transfer rates are normally accompanied by increased pressure losses in the flow over such surfaces. Thus, surface modification for better heat transfer is a tradeoff between augmented heat transfer rate and raised pressure drop.

One important application of modified heat transfer surfaces is that of cooling channels for gas turbine blades. One of the main criteria for aircraft engine design is to have a high thrust-to-weight ratio. To meet this requirement, the thermal performance/efficiency of gas turbine blades must be improved. An efficient strategy is raising the turbine's intake temperature. However, this approach may damage the turbine blades. To prevent damage and avoid blade melting, efficient cooling of turbine blades is essential. In turbine blade cooling, different techniques are applied for the various areas of the turbine blade. As demonstrated in Fig. 1(a–c), rib turbulators are often installed in serpentine passages and fin cooling is often applied in trailing edge sections. Impingement cooling is often used at the leading edge areas and dimples are normally placed in the tip areas of the blade. The relevant research concerning modified heat transfer surfaces was reported by Han [1].
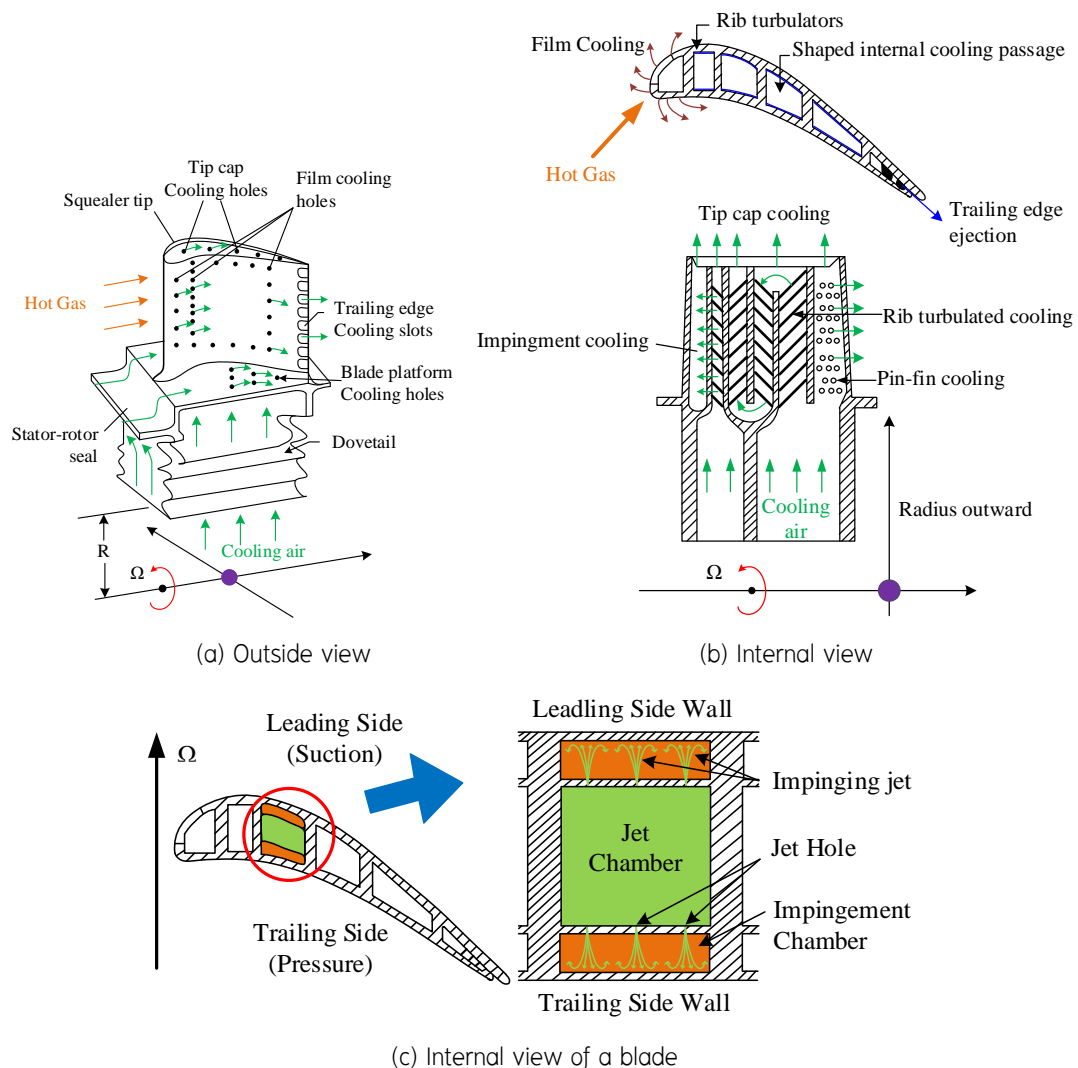

(a) Outside view

(b) Internal view

(c) Internal view of a blade

Fig. 1. Cooling of a gas turbine blade.

Due to the absorber plate and duct's poor heat transfer capabilities, the thermal performance of solar air heaters is commonly low compared to that of solar water heaters. Improvements in heat transfer coefficients will increase the performance of solar air heaters, making them more cost-effective. Rough elements should be placed only on the wall that collects solar radiation, since this is the only heated wall in solar air heaters, to maximize heat transfer. Solar air heaters are thus represented by a rectangular duct with one rough wall and three smooth side walls.

One way to collect the sun's warmth is with a solar air heater (Fig. 2). These systems have been used in a variety of heat transfer applications, including solar-powered agricultural drying processes, indoor heating and cooling, nighttime cooling, preheating ventilation makeup air, and timber seasoning. Laminar sublayers often develop above absorber plates and other heat-transfer surfaces to limit the amount of heat lost to the surrounding medium. Creation of a laminar sublayer reduces the energy-collecting performance of a solar air heating system because it leads to poor air-side heat transfer ability, absorber plates with high temperatures, and high heat losses to the environment. Heat transfer coefficients are a crucial parameter in solar air heating system design. This can be accomplished by incorporating artificial surface roughness on the solar collector at various orientations and shapes of the roughness. There are two strategies for maximizing heat convection from an absorber plate to the surrounding air. The primary method does not affect the heat transfer coefficient. It involves expanding the area of heat transfer through the utilize of corrugated/grooved or extended surfaces known as fins. The second approach generates surface turbulence, which improves heat transfer coefficient. The bottom surface of an absorber plate might be purposefully roughened for this purpose. Several researchers have worked to reduce frictional losses while increasing convective heat transfer using a roughened element.
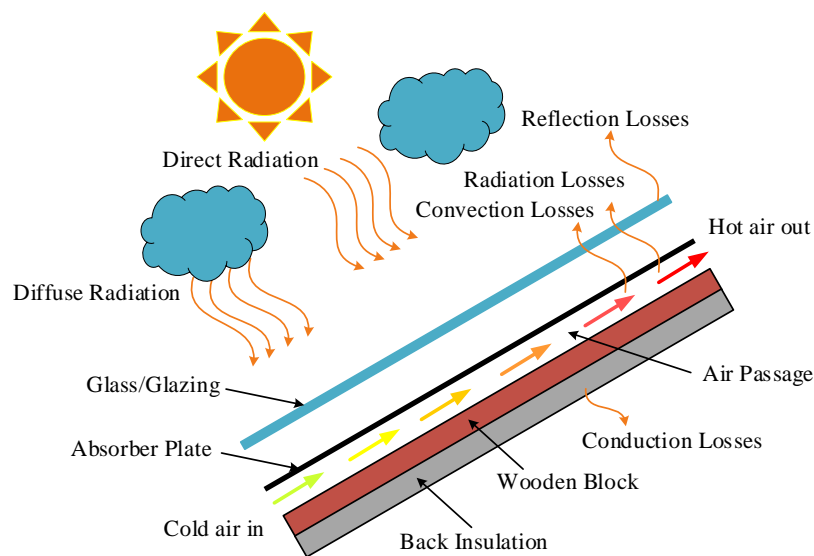

Fig. 2. Solar air heater.

Ribs and baffles are the major types of rough surfaces that have been widely developed and modified by many researchers. Flow through the ribs/baffles is extremely complex. There are several factors affecting heat transfer and pressure drop. In general, experimentation is time-consuming and expensive since it requires researchers to repeatedly test variations in a variety of variables. Another option is using numerical method. The advantage of numerical methods is that it allows researchers to examine issues that cannot be studied experimentally while permitting deeper research to investigate whether two or more variables are related. As previously stated, heat-transfer enhancement is obtained at the expense of an increased pressure loss.

Energy lost due to pressure losses may sometimes exceed that gained by heat-transfer enhancement. For many practical applications, it is necessary to determine the net economic benefit arising from a heat-transfer enhancement.

As depicted in Fig. 3, the present work concentrates on a review of the heat transfer enhancement technique using ribs and baffles in a channel with varying geometric characteristics. Using turbulence promoters and vortex generators to enhance the thermal performance of heat exchanger ducts, turbine blade cooling, and solar air heaters is the focus of this paper. The literature review focuses on the effect of shape parameters on heat transfer mechanisms, flow structure, pressure losses, and thermal performance characteristics, focusing on studies from the past to the present. All articles were searched for in the scopus and google databases for this analysis.
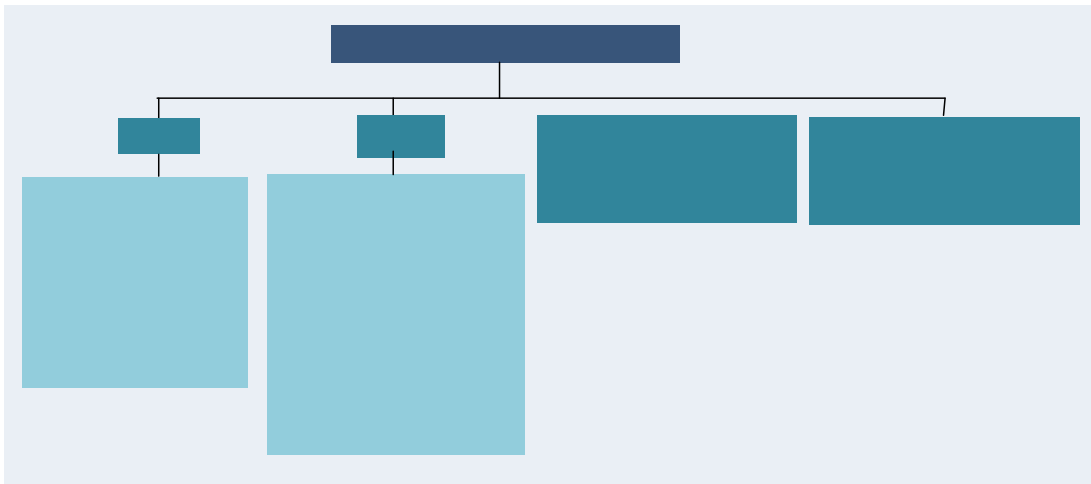

Fig. 3. Review of the heat transfer enhancement scope of the present work.

Rough surface Types	Three-dimensional roughened surface (consistency rough surface)	Two-dimensional roughened surface with protruding or convex surface	Two-dimensional roughened surface with grooves or holes
Common basic shapes			
Basic roughness shapes with modified distances between the rough protrusions			
Various rough surface shapes			

Fig. 4. Basic geometry of roughened surfaces [4].

2. Guidelines for designing roughened surfaces within channels

Applications of rib/baffle rows can greatly increase the convection coefficient over that of smooth surfaces since rough surfaces create recirculation/longitudinal-vortex flows that reduce the thin thermal layer thickness. This leads to a higher convection coefficient in the reattachment flow region. Optimization of ribs/baffles geometries plays a major part in enhancing the thermal performance factor, as it is influenced by crucial geometric parameters. These include rib thickness, rib arrangement and various designs adjusting the angle of flow attack (α), rib width (w), rib height (e) distance between ribs (p) and the rough surface shape. Numerous possible channel roughening geometries have been used to improve heat transfer rate. These are partially are compiled in Fig. 4. Three basic roughness groups can be identified, 3-dimensional, ridge type 2-dimensional and groove type 2-dimensional roughness. In designing ribs/baffles, geometric parameters usually take form of dimensionless variables such as the rib height ratio (e/d, BR), rib spacing ratio (p/e, PR), the ratio of the rib width (w/e) and the shape of the surface roughness, among others.

3. Thermal performance assessment

Many performance evaluation criteria (PECs) have been suggested by researchers for relative evaluation of heat transfer enhancement, but it is important to note that applicability varies depending on the specifics of the application [5–7]. Table 1 provides a preliminary listing based on the classification established by Bergles *et al.* [8] and its following revisions [5, 9]. Two of the most popular figures of merit for thermal hydrodynamic performance in the chemical and process industries are reviewed here to demonstrate this trade-off and provide optimization guidelines.

FG-2a: In the absence of enhancement, quantify the additional heat load Q induced by the technique when the geometry of the heat exchanger (N and L), the temperature difference across the approach (ΔT_i), and the pumping power P are all the same as the case with no enhancement. Heat load and pumping power can both be determined by reference to their commonly accepted definitions.

$$Q = \varepsilon(\dot{m}C_p)\Delta T_i \approx hA\Delta T = (\pi kLN\Delta T_i)Nu \tag{1}$$
$$P = (\dot{m}/\rho)\Delta p = (\pi\mu^2 L/2\rho^2 d^2)(fRe^3) \tag{2}$$

VG-1: When the mass flow rate, pumping power P, heat load Q, and approach temperature differential (ΔT_i) remain unchanged, as in the case with no enhancement, the surface area (A) of the heat exchanger is lowered by a quantifiable amount for the enhancement technique. It is noteworthy that the condition of a fixed pressure drop remains constant under the constraints of constant $\dot{m}$ and P values.

$$\Delta p = f(4L/d)(\rho V_o^2/2) = (2\mu^2 L/\rho d^3)(fRe^2) \tag{3}$$

In most enhancement technology applications, these figures of merit highlight the key design issues, which are maintaining greater heat loads in a given heat exchanger or decreasing the size of the heat exchanger for a offered heat load. Evaluating the enhanced thermal performance (or improvement in Q) owing to enhanced tubes in a heat exchanger under the constraint of fixed shape and equal pumping power is desirable in many applications involving chemical processing heat transfer or thermal manufacture of various fluid media. To do so, we can apply the FG-2a criterion described above and shown in Table 1, by writing the heat transfer rate for a duct/tube (Q_{tt}), with an insert, as a fraction of the heat transfer rate for a plain or unaugmented tube (Q_{st}).

$$(Q_{tt}/Q_{st}) = (Nu_{tt}/Nu_{st})_{N,L,d,P,\Delta T_i} \tag{4}$$

The following constraint is imposed by Eq. (2) on the operation of a heat exchanger under the given conditions when using constant pumping power:

$$(fRe^3)_{\text{tt}} = (fRe^3)_{\text{st}} \tag{5}$$

The presence of ribs or rough surfaces always simultaneously causes a desired heat transfer enhancement and an unwanted friction loss penalty. Increased friction losses leads to a need for higher pumping power, which impacts the economics of operation. Therefore, both effects need to be considered for evaluation of overall performance. Generally, improved heat transfer is determined in terms of a normalized parameter, the Nusselt ratio (Nu/Nu_s), where Nu is the Nusselt number in roughed channels/pipes and Nu_s is the Nusselt number in smooth channels/pipes. Similarly, increased friction losses are presented in term of a dimensionless friction factor ratio (f/f_s), where f is the friction factor in roughed channels/pipes and f_s is the friction factor in smooth channels/pipes. The overall performance of the operation is evaluated in terms of a thermal performance factor (TPF). Fundamentally, the TPF is a ratio of the convection coefficient in roughened channels/pipes (h) to that of smooth channels/pipes (h_s). Under identical pumping power conditions, the convection coefficient ratio can be written in terms of the Nusselt number and friction factor ratios as shown in Equation (1) [10–14].

$$TPF = \left.\frac{h}{h_s}\right|_{\text{pp}} = \left.\frac{Nu}{Nu_s}\right|_{\text{pp}} = (Nu/Nu_s)/(f/f_s)^{\frac{1}{3}} \tag{6}$$

According to Equation (6), a high thermal performance factor (TPF) can be achieved by enhancing heat transfer while controlling friction losses so that they are as low as possible.

Table 1: Standards for evaluating performance of tubular heat exchangers utilizing single–phase forced convection [6].

Case	Shape	W	P	Q	ΔT_i	Aim
FG–1a	N,L^a	x			x	$\uparrow Q$
FG–1b	N,L	x		x		$\downarrow \Delta T_i$
FG–2a	N,L		x		x	$\uparrow Q$
FG–2b	N,L		x	X		$\downarrow \Delta T_i$
FG–3	N,L			x	x	$\downarrow P$
FN–1	N	x	x	x	x	$\downarrow L$
FN–2	N	x		x	x	$\downarrow L$
FN–3	N	x		x	x	$\downarrow P$
VG–1		x	x	x	x	$\downarrow NL$
VG–2a	N,L^b	x	x		x	$\uparrow Q$
VG–2b	N,L^b	x	x	x		$\downarrow \Delta T_i$
VG–3	N,L^b	x	x	x	x	$\downarrow P$

† According to Bergles's [5] classification.   * The product of N and L.

4. Enhancing heat transfer with ribs

The flow of a viscous fluid in a plain pipe will result in a non-uniform velocity distribution across the pipe cross-section. The fluid velocity near the wall of the pipe is very low, which is significantly different from that at the pipe core. Alternatively, the flow of non-viscous fluid (inviscid flow) usually shows a uniform velocity distribution. In case the fluid flowing through a two- or three-dimensional rough pipe, different velocity distribution patterns are generated depending on the base geometry of surface roughness. Flow behaviors consequently affect the heat transfer rate in the pipe or channel. Figs. 3 and 4 illustrate the flow behavior through single rib and continuous ribs by the hydrogen bubble technique in a channel at the low Reynolds number [15]. The flow pattern at the inlet of the channel is a fully deveopled flow. Flow velocity is dependent on the radial distances from the pipe wall. Flow velocity is zero at the wall. The flow reaches maximum velocity at the pipe core. Collision between the fluid and ribs results in flow separation and eddy motion or vortices behind the rib. The size and shape of the vortices are dependent on surface roughness. For a single rib, the flow begins to develop into one that is fully developed after passing the rib at a certain distance, as display in Fig. 5(a). To maintain the secondary flow or flow disturbance, a series of ribs must be applied as demonstrate in Fig. 5(b). This results in a decreased thickness of the velocity boundary layer and increased heat transfer [16] as depicted in Fig. 6. However, the spacing between the ribs must be appropriately designed as described in the next section.

flow in

(a) Flow behavior over a single rib at a Reynolds number of 490

flow in

(b) Flow behavior over a pair rib in series at a Reynolds number of 490
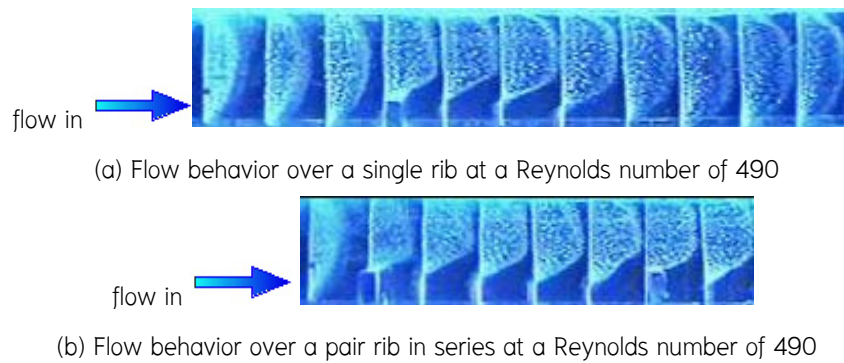
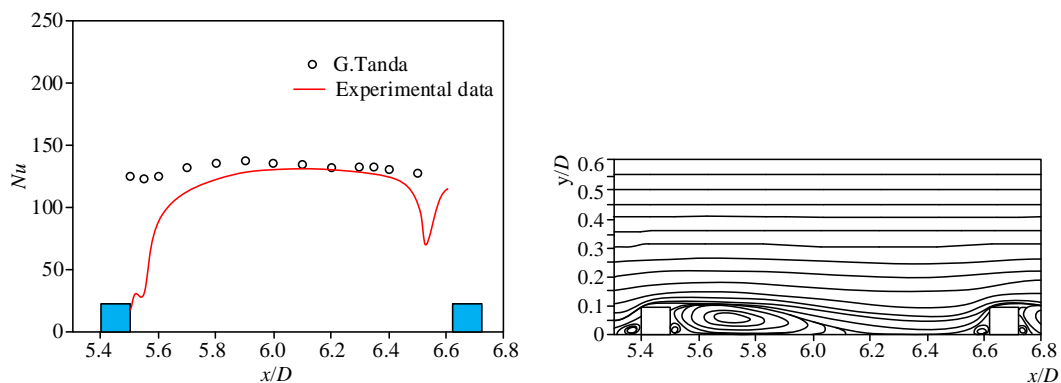**Fig. 5.** Flow behavior aver rib (s) observed *via* the hydrogen bubble technique [15].

Fig. 6. Local Nusselt number distribution (upper figure) and streamline distribution (lower figure) in a channel with continuous ribs [16].

The flow pattern is dependent on the shapes/geometries of the rough surfaces. Generally, recirculation flow (eddy motion) usually takes place adjacent to the rear of modified surfaces, followed by flow reattachment, which directly promotes heat transfer [17, 18], as shown in Fig. 7(a). Figures 7(b) and (c) illustrate the temperature and Nusselt number gradients throughout the

direction of flow, respectively. The temperature of the fluid increases as the result of heat transfer rate from the channel wall. Here, the Nusselt number reaches a periodic condition at around the 5th rib. The number of ribs within the channel also has a role in the onset of a periodic condition. The major parameters that affect the heat transfer rate and pressure loss in a system with ribs are the Reynolds number, rib shape/design, attack angle of the ribs, rib height, rib arrangement, ribs with special design (baffles).
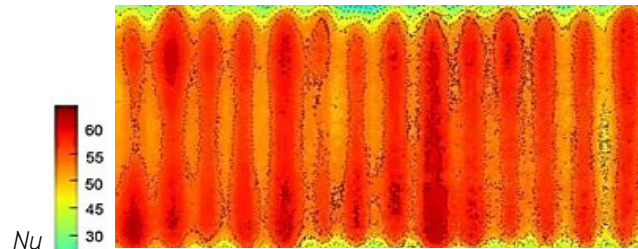
(a) Nusselt number contour in the channel with continuous baffles [17]
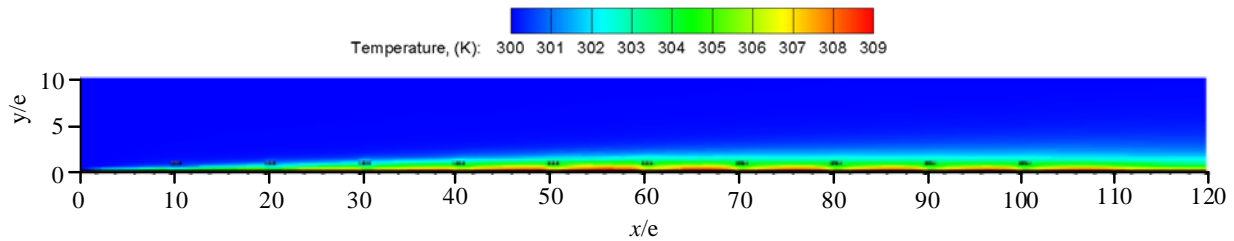
(b) Temperature contours in a channel with continuous ribs [18]
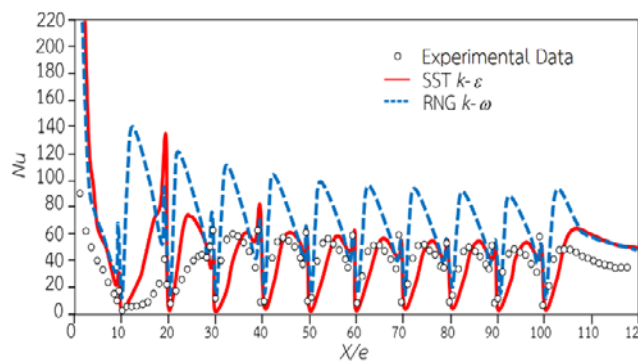
(c) Comparison of experimental and numerical results of Nusselt number distributions in a channel with continuous ribs [18].

Fig. 7. Nusselt number and temperature contours in a channel with continuous ribs.

4.1 Effect of Reynolds number

The Nusselt numbers grow as the Reynolds numbers rise due to the thinning thermal boundary layer and thus, reduction of convective resistance. Simultaneously, an increased Reynolds number helps to decrease the friction factor since a greater Reynolds number diminishes the viscous boundary layer. Recirculation behaviors between ribs at Reynolds numbers (Re) of 100 and 1000 are shown in Fig. 8. The greater the Reynolds number, the size and amplitude of the eddy currents are promoted and the thermal boundary layer becomes thinner [19]. This is supported by that data in Fig. 9, which shows that the Nusselt numbers at Re = 20,000 are significantly higher than those at Re = 4000 [17]. Additionally, Fig. 9 also indicates that a high Nusselt number region is located midway between each pair of ribs, where flow reattachment takes place.
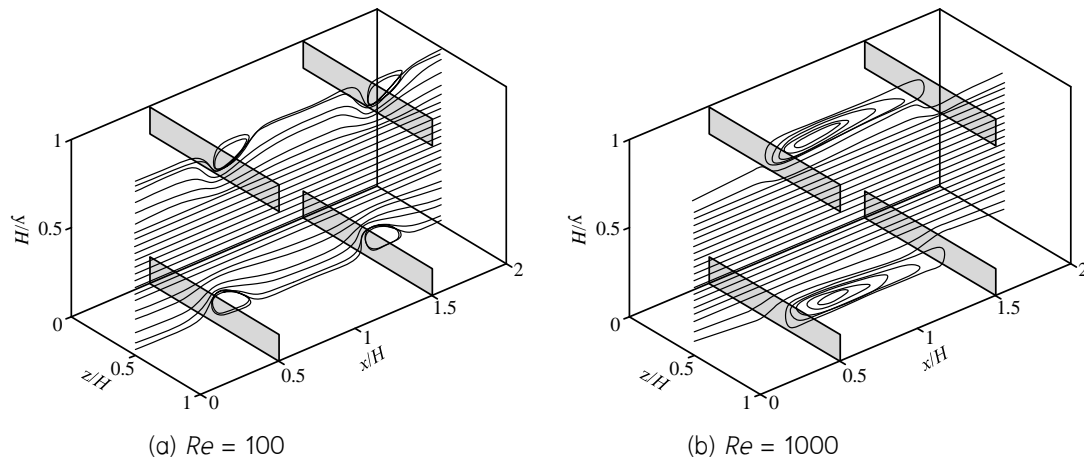
(a) *Re* = 100 (b) *Re* = 1000

Fig. 8. Recirculation flow behavior between ribs at various Reynolds numbers [19].
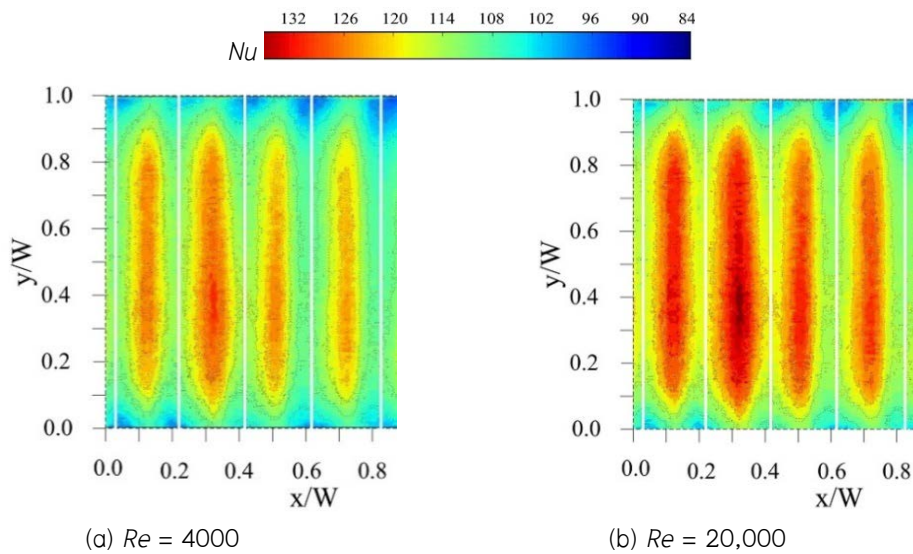

(a) *Re* = 4000 (b) *Re* = 20,000

Fig. 9. Effect of Reynolds number on heat transfer behavior in a ribbed channel [17].

4.2 Effect of rib shape/design

Rib shape and design significantly influence the heat transfer behavior and flow structure in ribbed pipes and channels. Generally, ribs cause separation and reattachment flows on heat transfer surfaces. Both improved heat transfer rate and higher pressure loss result from the phenomenon at the same time. Numerous researchers have modified ribs for better tradeoffs between these effects. Nuntadusit *et al.* [20] developed the straight perforated rib shown in Fig. 10(b), and an inclined perforated rib shown in Fig. 10(c). They compared their performance with that of a conventional solid rib (Fig. 10(a)).

(a) Solid rib (b) Straight perforated rib (c) Inclined perforated rib
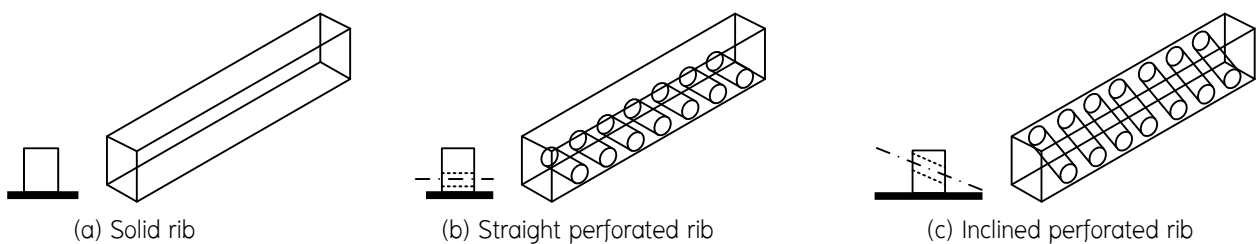
Fig. 10. A conventional solid rib and modified ribs [20].

The numerical results in Fig. 11 suggest that a solid rib causes a long separation flow behind the rib. Alternatively, the holes as part of the straight perforated ribs and inclined perforated ribs direct jets on the heat transfer surfaces behind the ribs as depicted in Figs. 11(b–c). This allows for more efficient local heat transfer compared to the conventional solid rib design. Additionally, an inclined perforated rib gives a stronger attack angle and thus higher Nusselt number than an uninclined rib.
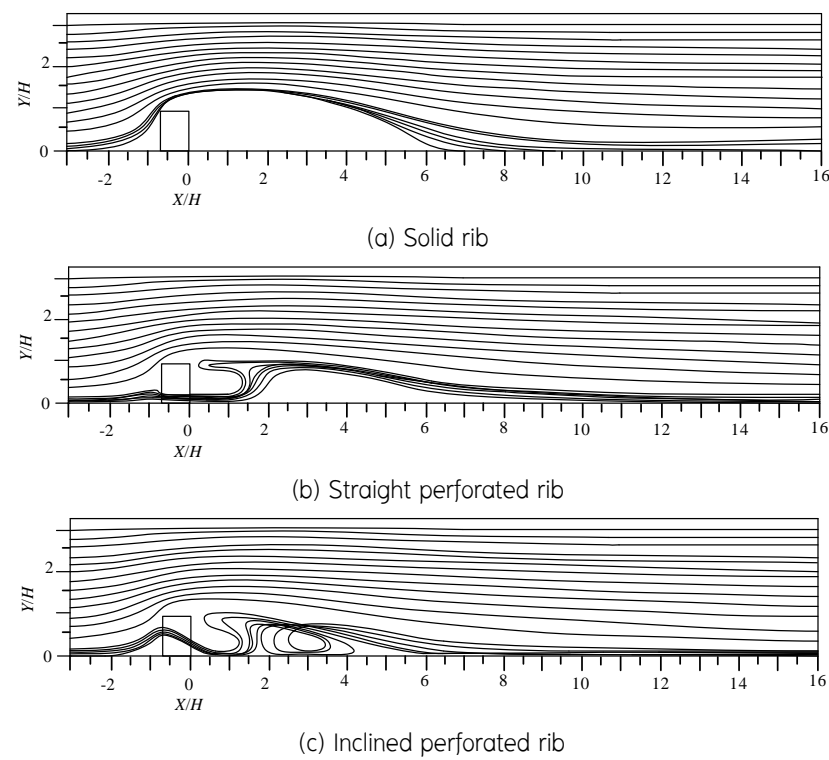
(a) Solid rib

(b) Straight perforated rib

(c) Inclined perforated rib

Fig. 11. Post–rib flow and heat transfer behavior at a Reynolds number of 60,000 [20].

In Fig. 12, we can see how various ribs improve heat transfer rate. Clearly, inclined perforated ribs with a larger perforation angle (30°) yield better heat transfer adjacent to a rib than is observed with a smaller angle (15°). However, all perforated ribs yield comparable heat transfer in the reattachment region.
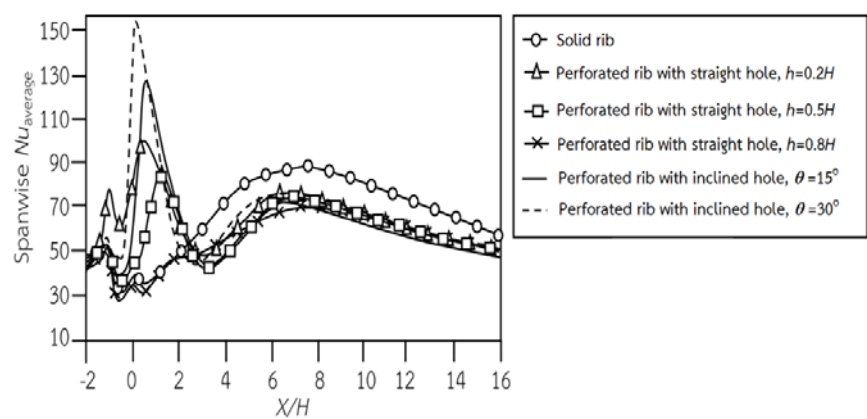
Fig. 12. Nusselt numbers distribution in the channels with different types of ribs [10].

Additionally, Changcharoen and Eiamsa-ard [21] studied the flow behavior of uplifted ribs (detached ribs), as shown in Fig. 13. Rib detachment has a substantial influence on the flow pattern. Separated ribs allow fluid flow to reach the height gap. As can be seen in Fig. 14, the flow has an immediate effect on the thickness of the thermal boundary layer, which in turn increases heat transfer. Subsequent flow reattachment leads to maximal heat transfer area. Yongsiri *et al.* [18] developed ribs with various inclination angles. The fluid flow direction corresponds to the inclination angles, as shown in Fig. 15. The presence of rib gaps also helps in decreasing the pressure loss of the system. Jiang and Gao [22] reported the heat transfer mechanism and flow pattern in ducts with 45°/60°/75° V-shaped and 45°/60°/75°/90° parallel ribs. They showed that the duct rough with 45° V-shaped ribs was found to have the greatest longitudinal secondary flow regions and the largest mainstream secondary flow regions.

(a) *c/a* = 0.0   (b) *c/a* = 0.2
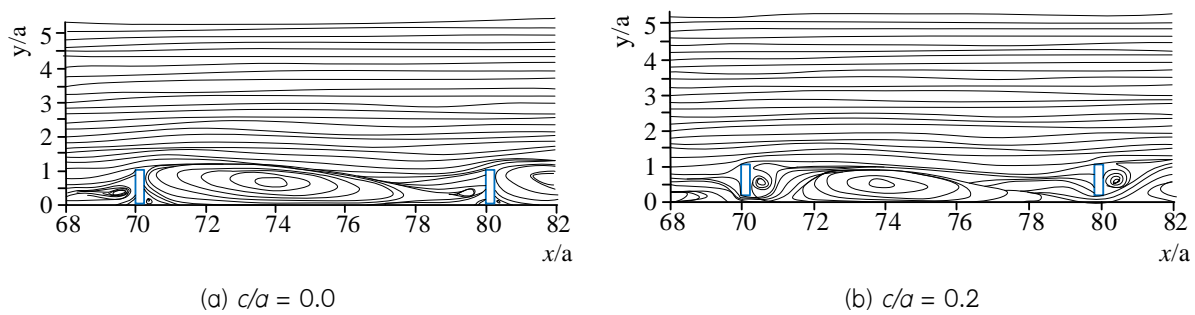
Fig. 13. Flow behavior in the channel with uplifted (detached) ribs at a Reynolds number of 8000 [21].
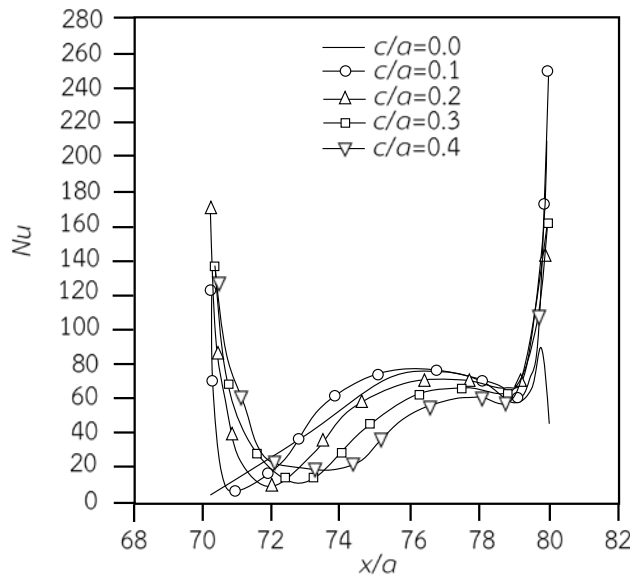

Fig. 14. Heat transferf distribution (*Nu*) in a channel with detached ribs installed at *Re* = 8000 [21].
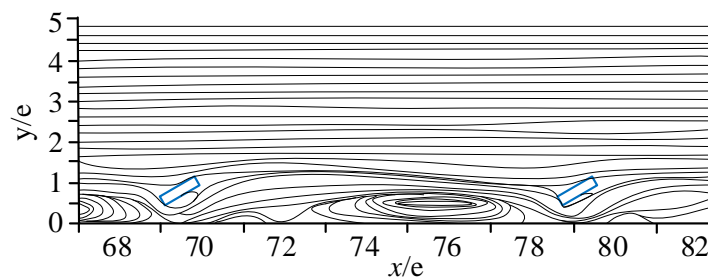

Fig. 15. Flow behavior in a channel between the 7th and 8th ribs for detached ribs with a 150[o] attack angle [18].

Ribs commonly have two major forms, protruding and grooved (or a combination of these two types of roughness), as shown in Fig. 16. Their geometries can be varied by changing the height (or depth) and width of the protrusion or groove. A change of rib geometry directly affects the heat transfer mechanism and flow pattern of enhanced systems as the sample numerical results in Fig. 17. Generally, the surface friction coefficient increases as the groove width decreases, as depicted in Fig. 18.
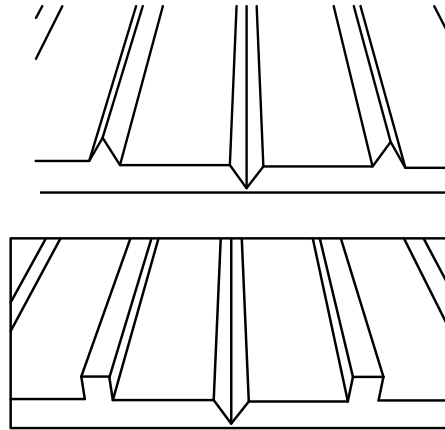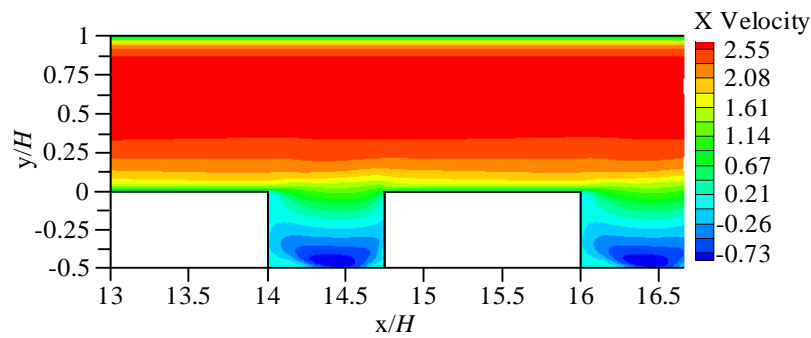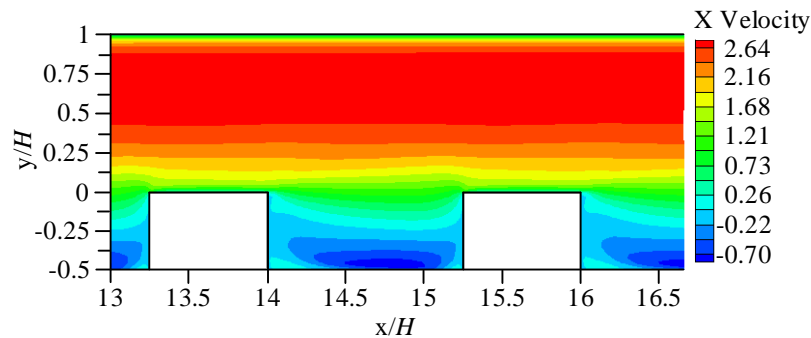

Fig. 16. Illustration and imagery of grooved ribs [23].

(a) *B/H* = 0.75

(b) *B/H* = 1.25

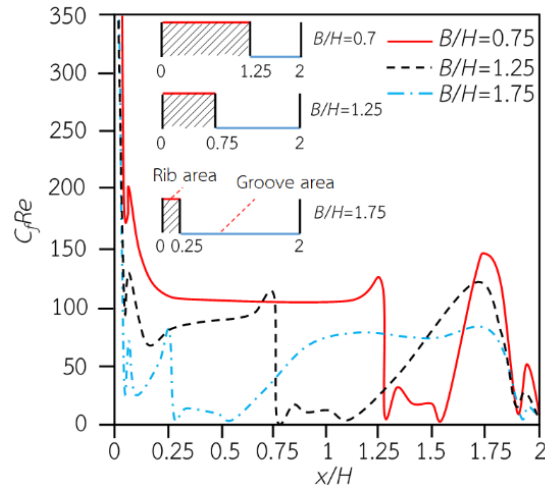**Fig. 17.** Influence of groove width on heat transfer [24].

Fig. 18. Influence of groove width on surface friction coefficient distribution [24].

Triangular prism ribs are another type of rib that are applied for heat transfer augmentation. Numerical results by Eiamsa–ard *et al.* [25] reveal that triangular prism ribs introduce turbulent eddy flows as display in Fig. 19. Adjusting the location of the prism affects the distribution of the Nusselt numbers, as depicted in Fig. 20. Prism ribs with a small clearance ratio ($CR = 1.5$) induce a high Nusselt number area near the ribs, according to the location of the reattachment flow [25]. However, ribs with a large clearance ratio ($CR = 3.0$) cause long flow separation behind the ribs. Therefore, the high Nusselt number area related to the reattachment location shifts downstream. It is notable that at $CR = 3.0$, the reattachment area is larger than that found at $CR = 1.5$. Ribs with various shapes/arrangements lead to different attack angles of flows, which directly affect flow and heat transfer characteristics. Numerical results of Eiamsa–ard and Changcharoen [16] reveal that a reduction of rib sharpness helps in suppressing sudden changes of the main flow and flow separation, as display in Fig. 21. Consequently, the hot spots behind the ribs become smaller, especially with concave–concave ribs, as demonstrated in Fig. 22. Additionally, the results of Eiamsa–ard and Chuwattanakul [17] indicate that the utilize of inclined ribs with a low *p/w* yield greater heat transfer than for a higher *p/w* as seen in Fig. 23.
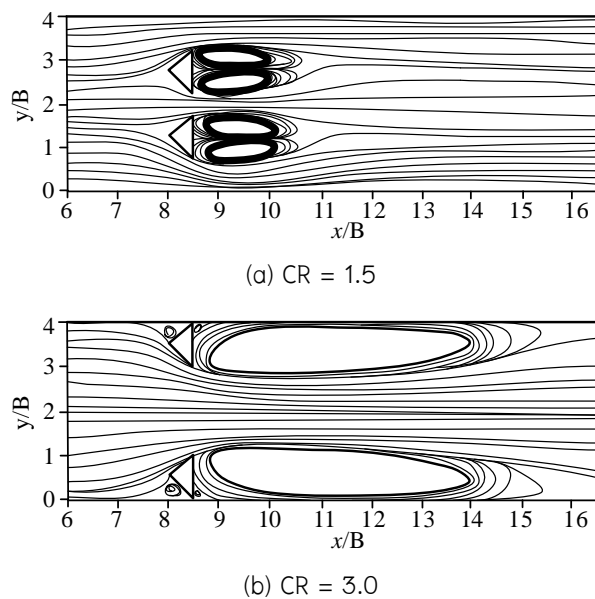

(a) CR = 1.5

(b) CR = 3.0

Fig. 19. Streamlines in channels equipped with a triangular prism at various clearance ratios [25].
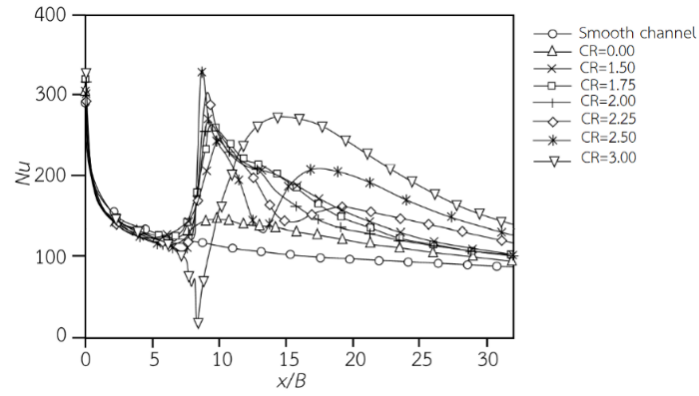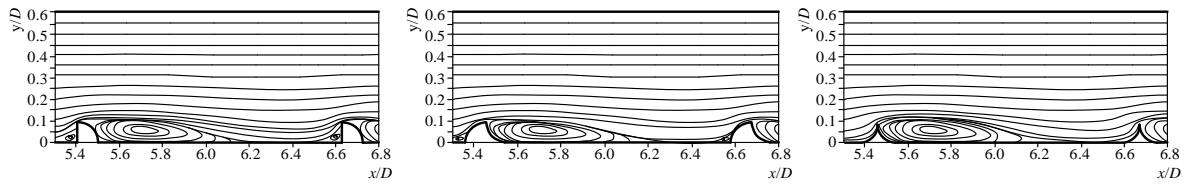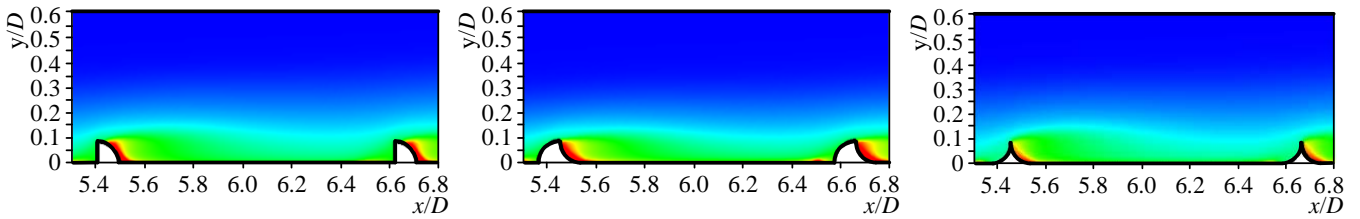
Fig. 20. Axial distribution of *Nu* on the bottom wall surface of the channel at *Re* = 20,000 [25].
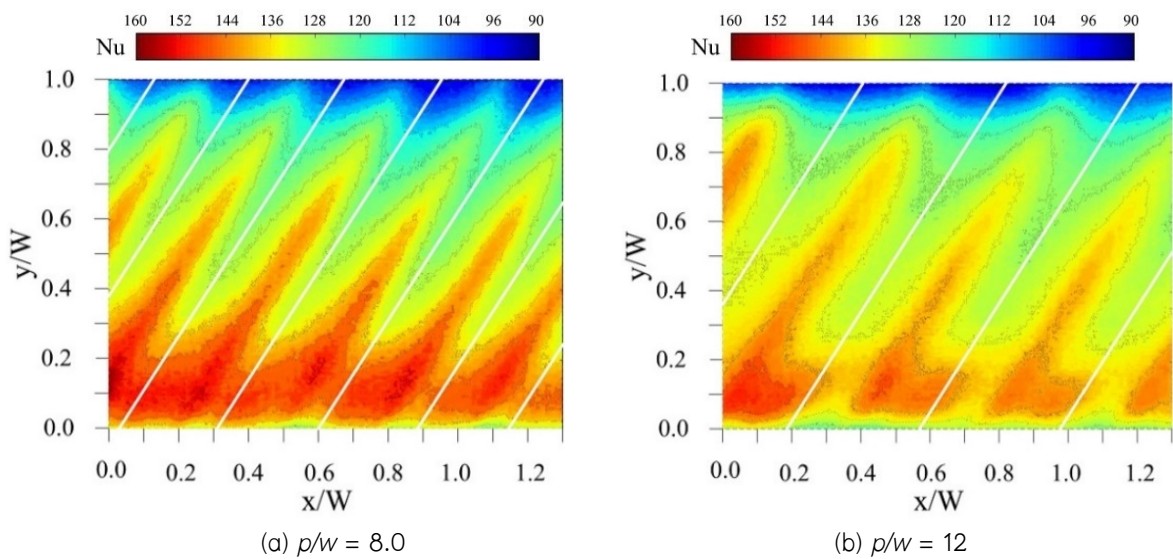

(a) Downstream convex ribs   (b) Convex–concave ribs   (c) Concave–concave ribs

Fig. 21. Effects of various curved ribs on flow characteristics at *Re* = 25,000 [16].

(a) Downstream convex ribs   (b) Convex–concave ribs   (c) Concave–concave ribs

Fig. 22. Effects of various curved ribs on temperature distributions at *Re* = 25,000 [16].

(a) *p/w* = 8.0   (b) *p/w* = 12

Fig. 23. Nusselt number distribution in an inclined baffled channel at *Re* = 20,000 [17].

Heat transfer in a channel with a wide range of rib shapes was studied by Wang and Sundén [26]. The pitch-to-height ratios of these ribs ranged from 8.0 to 15.0. Real-time Laser Holographic Interferometry tests were performed in $8,000 \leq Re \leq 20,000$ to measure the average and local heat transfer. They discovered that ribs with a trapezoidal shape transferred heat more effectively than ribs of other shapes. Heat transfer and pressure drop characteristics were investigated by Xie et al. [27], who evaluated the influence of truncated rib and mid-truncated rib, offset position, and angles. They found that the pressure loss was minimal when the ribs were truncated at 90 degrees in the middle and placed without any offset, while 135° mid-truncated ribs provided the greatest heat transfer coefficient. The enhanced heat transfer rate was tested by Iacovides et al. [28] in a duct with staggered ribs. Local heat transfer was demonstrated utilizing a thermochromic liquid crystal (TLC) sheet. Average fluid motion and its fluctuations were estimated using laser Doppler Anemometry. They noticed that the structure of the flow and the local heat transfer varied considerably over the length. Secondary flows and recirculation influenced flow and thermal developments. According to Mahanand and Senapati [29], quarter-circular ribs (Fig. 24) offered the highest thermal enhancement factor, 1.88. Triangular ribs performed the best heat transfer rate, according to Ekiciler and Çetinkaya [30], who used elliptical, square, and triangular shaped transverse ribs (Fig. 25) for heat transfer enhancement. Liu et al. [31] improved heat transfer and the thermal enhancement by altering conventional transverse ribs to create truncated ribs (Fig. 26). They revealed that the truncated ribs promoted reduced pressure losses without negatively impacting heat transfer. According to Liu et al. [32], perforated transverse ribs (Fig. 27) can increase heat transfer by 4-8% while decreasing pressure losses by 12-24% compared to traditional ribs.
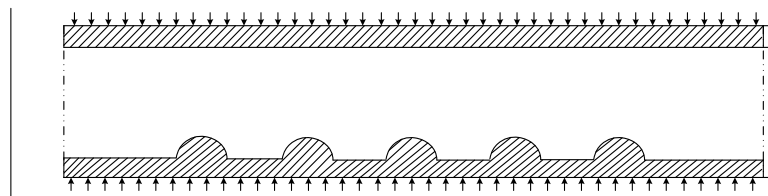

Fig. 24. Quarter-circular ribs [29].

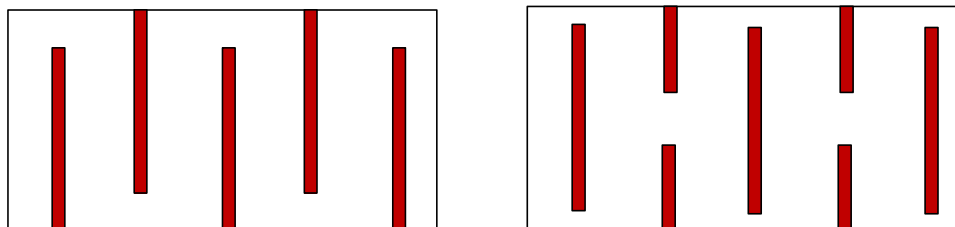**Fig. 25.** Transverse ribs with ellipses [30].

Fig. 26. Truncation ribs [31].

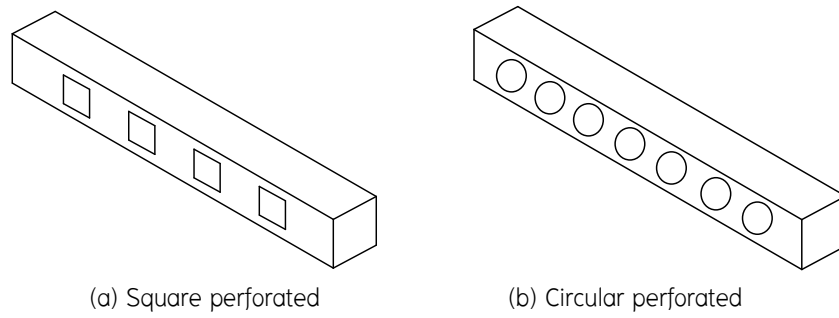(a) Square perforated (b) Circular perforated

Fig. 27. Perforated transverse ribs [32].

4.3 Effect of rib height

The thickness of the boundary layer and the rate of heat transfer are both directly affected by rib height. Generally, increased rib height introduces stronger turbulence/reattachment and superior heat transfer. However, further increased rib height beyond the appropriate level leads to the absence of reattachment (Fig. 28) and thus, poorer heat transfer rate due to the flow patterns [33]. The analysis by Prasad and Saini [34], suggests that the optimum rib height is slightly larger than the transition sublayer thickness. Under this condition, ribs noticeably enhance heat transfer with moderate pressure losses since they do not protrude into the turbulent core. Alternatively, excess rib height causes a high pressure drop penalty that directly degrades thermal performance. Figs. 29 and 30 show that eddy currents or recirculation flow occurs adjacent to the rear of a rib. As the rib height to channel height ratio (BR) grows larger, the size and shape of the eddy currents become larger. Consequently, the reattachment areas shrink. Therefore, excessively high ribs are used, leads to inefficient heat transfer [19, 35].

Fig. 28. Effect of rib height in terms of rib height to channel diameter ratio (*e/D*) on flow patterns [33].

Promvonge *et al.* [36] investigated the turbulent flow in a duct with thin discrete inline 60° V-shaped ribs. According to their findings, a pair of counter-rotating vortices (P-vortices) were created by the ribs, and these P-vortices triggered impingement flows that improved heat transfer. With increasing blockage ratio, pressure losses and heat transfer increased. Ribs with a blockage ratio value of 0.0725 at *Re* = 10,000 produced the highest thermal performance factor, 1.8. As much as four times as much heat was transferred in this configuration as in a square, smooth duct. According to Bahiraei *et al.* [37], the increase in the heat transfer coefficient was caused by reducing rib pitch and increasing rib height. It can be concluded from the above results that there is an appropriate range of rib height which offers efficient heat transfer with a reasonable pressure loss penalty. Since it is related to the reattachment flow [38–40], the roughness height ratio (e/D_h) has a substantial influence on the flow and heat transfer of enhanced thermal systems.
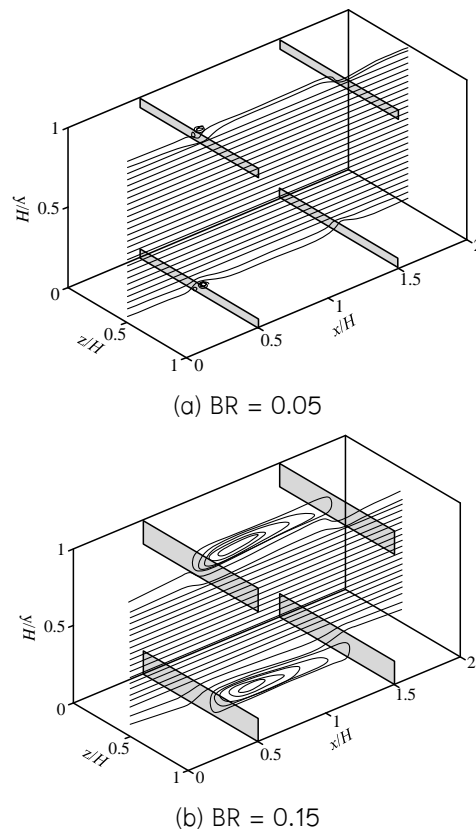

(a) BR = 0.05

(b) BR = 0.15

Fig. 29. Flow patterns in a ribbed channel with different rib heights [19].
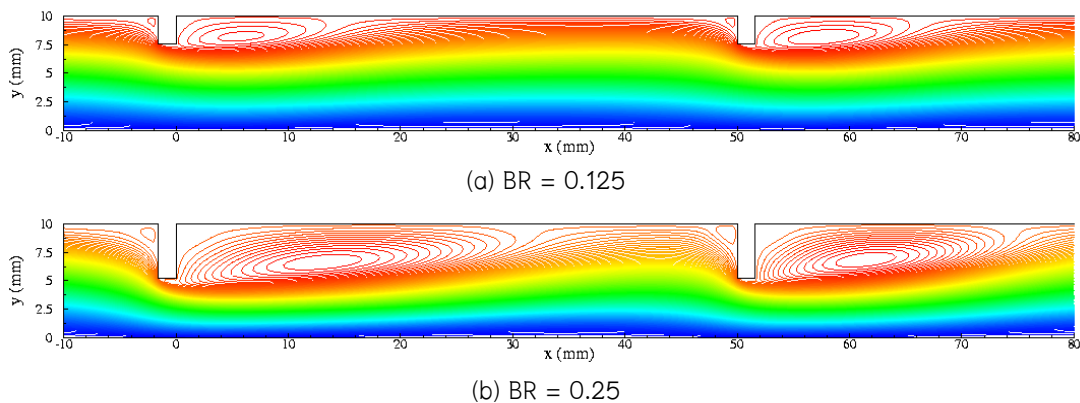

(a) BR = 0.125

(b) BR = 0.25

Fig. 30. Prediction of flow in a ribbed channel with different rib heights [35].

p/e	Flow pattern between ribs
∞	
10	
6.0	
5.0	
2.0	
0.75–1.25	

Fig. 31. Effect of rib pitch on downstream flow [33].

4.4 Effect of rib pitch

Creating an artificially rough absorber plate bottom for a solar air heater duct, the heat transfer coefficient between the absorber plate and the air can be significantly enhanced. The effect of relative pitch (*p/e*) on heat transfer rate and pressure loss in a roughened duct of varying form roughness geometries was investigated experimentally [41–45]. Prasad and Saini [34] present the flow patterns associated with ribs having different pitch ratios (*p/e*) as seen in Fig. 31. Reattachment of a free shear layer appears at 6e–8e, behind each rib. Therefore, installing ribs at pitch ratios (*p/e*) values smaller than 6 leads no reattached flow. Consequently, the heat transfer rate is reduced to levels even poorer than that of smooth surface in some cases. Additionally, decreasing rib pitch monotonically increases friction losses. Therefore, ribs having *p/e* values less than 6.0 yield extremely low thermal performance. Alternatively, ribs with excessive pitch values yield low heat transfer and thus, low thermal performance due to inconsistent reattachment. Generally, optimal rib pitches producing maximal thermal performance, are in the range of 6.0 to 10.

Yadav and Bhagoria found that the transverse ribs at various shapes as see in Figs. 32–34 that significantly boost the degree of turbulent flow closer to the heat transfer surface [46–48]. Aharwal *et al.* [49] looked at the way a solar air heater worked when it used ribs that were repeated to improve the efficiency of the heater's heat transfer. They determined that the pressure loss reduction and heat transfer rate improvements over a smooth channel were 2.6% and 2.9%, respectively. It was determined that the optimum location and width ratios for thermal performance were 0.25 and 1.0, respectively. Gap width and gap position are two geometric variables that have been studied by Aharwal *et al.* [50]. They found that the pressure losses

increased to a value 3.6 times greater than that of a smooth channel, with a maximum increase in heat transfer that was 2.83 times that of a small channel at corresponding gap positions and pitch ratios of 1.0 and 8.0.
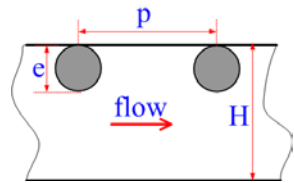

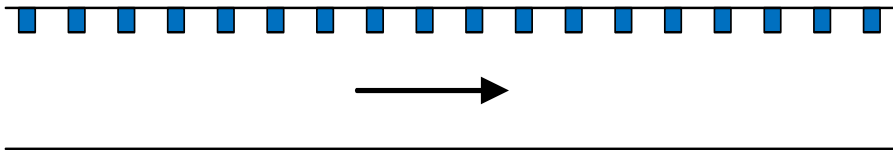**Fig. 32.** Circular ribs at p/e = 7.14–35.71, e/D = 0.021–0.042 [46].

Fig. 33. Rectangular ribs at p/e = 7.14–35.71, e/D = 0.021–0.042 [47].

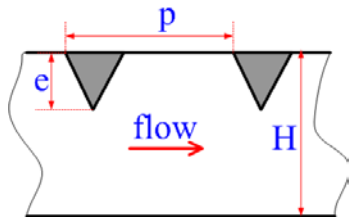**Fig. 34.** Triangular ribs at p/e = 7.14–35.71, e/D = 0.021–0.042 [48].

4.5 Effect of V–shaped/inclined ribs

There are two major categories of rib types. They are transverse ribs, which are arranged perpendicular to the flow, and V–shaped/inclined ribs, which are angled to the flow as shown in Fig. 35. Owing to their lower pressure losses, V–shaped ribs usually yield higher thermal performance (evaluated from $(Nu/Nu_s)/(f/f_s)^{1/3}$) than transverse ribs. Multiple V–shaped ribs are another form of V–rib modification (Fig. 35(c)), which introduce multiple pairs of eddy flows downstream of the ribs. These flows help in disrupting thermal layers and blending cold and hot fluids, resulting in enhanced heat transfer [51–53]. Generally, multiple V–shaped ribs cause fluid to impinge at the rear of ribs producing counter–vortex–flow as shown in Fig. 36. Flow leads to strong turbulence signified by high kinetic energy dissipation in the transverse flow plane. The impinged area shows excellent heat transfer since the cold fluid near the upper wall is induced by a recirculation stream to absorb heat from the hot lower wall and vice versa. In other words, the counter–vortex–flow promotes fluid mixing and thus, heat transfer.
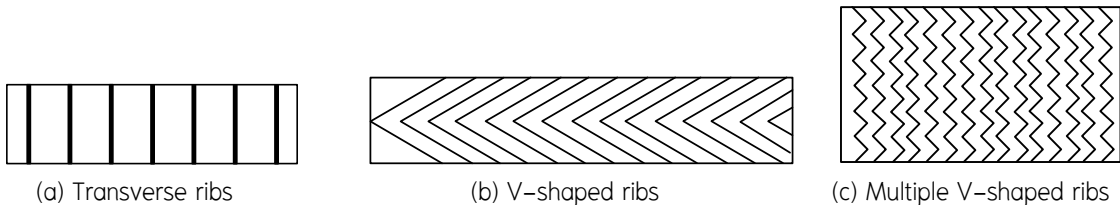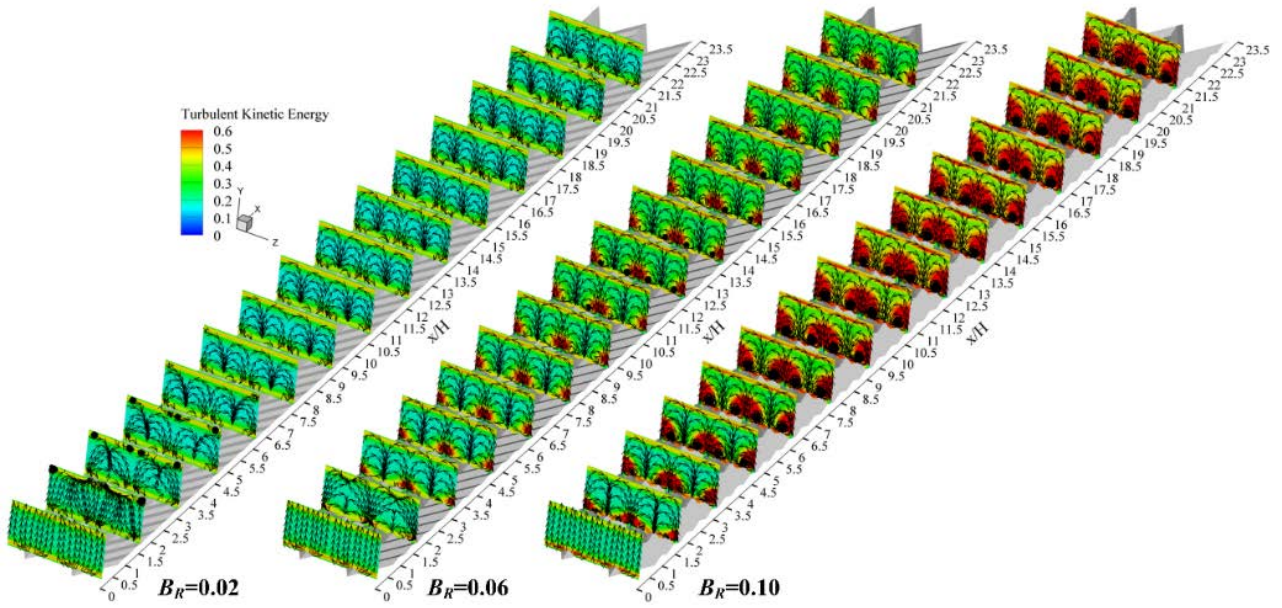

(a) Transverse ribs   (b) V–shaped ribs   (c) Multiple V–shaped ribs

Fig. 35. Transverse rib and V–shaped ribs/multiple V–shapes ribs [53].

(a) Streamlines and kinetic energy dissipation in the transverse flow plane
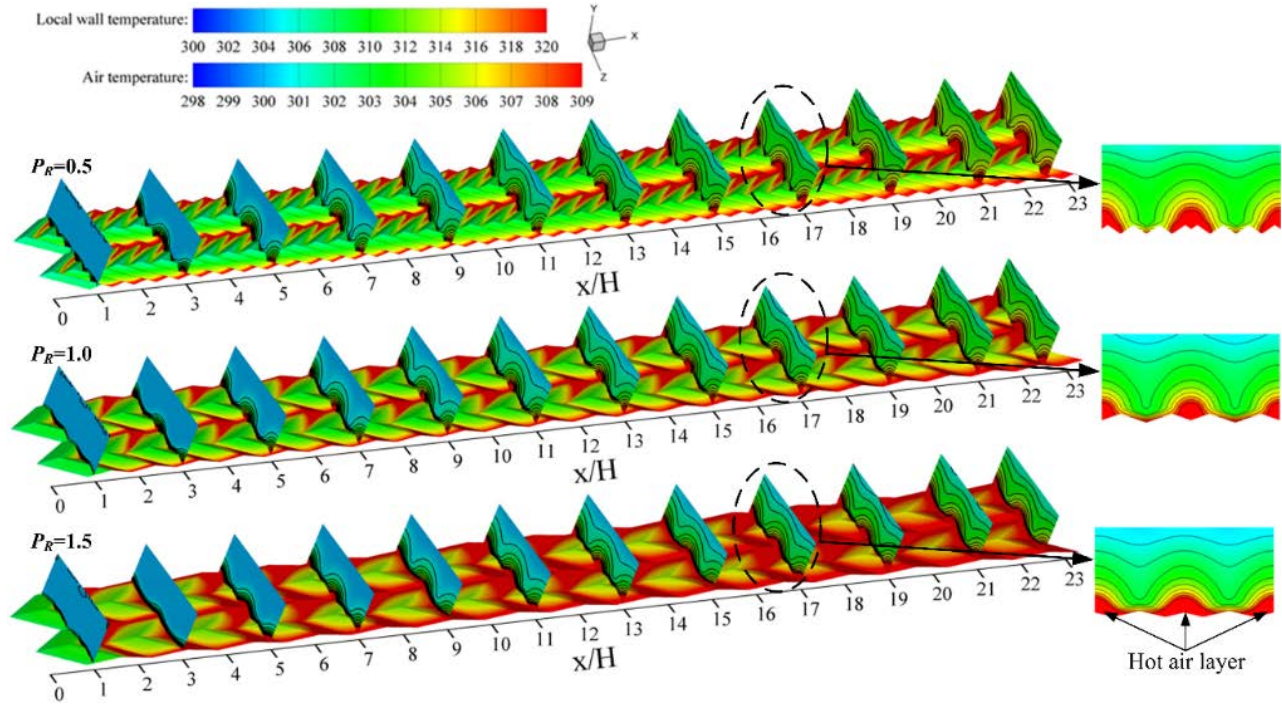
(b) Fluid and surface temperatures

Fig. 36. Flow behaviors and temperature distributions in a duct with multiple V-shaped ribs [54].

In a channel with inclined ribs, Chaube *et al.* [55] indicated increased heat transfer rate and pressure losses. Ribs with an attack angle of 60 degrees, a position ratio and a width ratio of 0.33 and 0.33 generated the highest heat transfer and pressure losses. Kaewchoothong *et al.* [56] examine how different arrangements of inclined angle ribs in a duct influenced local heat transfer. Based on their experimental findings, heat transfer by transverse ribs was respectively enhanced by about 20%, 25%, and 30% for inclination angles of 60°, 45°, and 60°. Experiments on heat transfer in a square channel with ribs on two walls were undertaken by Han *et al.* [57]. Researchers explored to see how rib arrangement affected performance. Heat was transported more efficiently with 'V' and angled ribs compared with continuous ribs. Among the angled ribs, the 60° angle ribs had the highest-pressure loss and heat transfer rates. Han *et al.* [58] also indicated that heating only one or both of the ribbed walls might very well increase

heat transfer efficiency compared to heating all four channel walls. Xie *et al*. [59] undertook a numerical analysis of the influence of rib arrangement on heat transfer and pressure losses. They compared a variety of configurations: continuous ribs of the same size, half-sized and same-size ribs below greater ribs, and half-size ribs between two larger nearby ribs. Their findings demonstrated that positioning the downstream ribs was an effective way to reduce pressure losses and enhance the flow structure. The thermal performance and heat transfer increase of different V-pattern ribs were evaluated by Kumar and HoeKim [60]. V-shaped ribs, protruding V-shaped ribs, dimpled V-shaped ribs, and grooved V-shaped ribs were all displayed. The best thermal performance was seen for ribs arranged in a V pattern with both grooves and rough surfaces.

Using a square channel with either V-ribs (V-shaped ribs with a 45° apex angle, with the apex pointing in the upstream and downstream directions) or W-ribs (W-shaped ribs with a 45° apex angle, with the central apex pointing in the upstream and downstream directions), Abraham and Vedula [61] investigated the characteristics of pressure drop and heat transfer enhancement. The experiments examined three relative pitch ratios (p/e = 6, 10, and 17.5). They found that compared to W-rib turbulators, V-rib turbulators offered higher heat transfer coefficients. Based on the thermal performance criteria for constant pumping power, the ideal condition was found using W-rib turbulators with a pitch ratio of 10. Han and Zhang [62] investigated the effects of broken V-ribs and continuous ribs in a square channel. They discovered that V-ribs with breaks at a 60-degree angle outperformed continuous ribs. A duct installed with 60° broken V-ribs provided up to 4.5 times more heat transfer than a channel without ribs. Using attack angles of $0°$–$165°$, Yongsiri *et al*. [18] studied how incorporating inclined detached-ribs to a channel improved heat transfer. Attack angles of 60° and 120° on the ribs were used in most of the testing. They generated the highest heat transfer and thermal performance indices. Karwa [63] evaluated how installing V-discrete ribs to a channel's wall increased heat transfer. The V-down discrete arrangement was found to have the best thermal performance of the geometries tested. Tanda and Abram [64] observed that the inclined ribs placed on one or both channel walls raised the transfer of heat rates. They noticed that the Nusselt number was 29% higher when inclined ribs were inserted on both sides of the channel, and the pressure loss was 3.0 times higher than in a smooth channel.

4.6 Summary of ribs

The most important characteristics of a rib's design and arrangement are its shape/design, its height, and its pitch. A designed rib may assume a variety of shapes and orientations. The previous section analyzes flow characteristics with respect to various types of rib features (solid ribs, straight perforated, inclined perforated, detached, grooved, triangular prism, downstream convex, convex-concave, concave-concave, downstream convex, convex-concave, concave-concave, staggered, truncated, elliptical shaped transverse, triangular shaped transverse, circular, V-shaped, and multiple V-shaped ribs, as well as V-pattern ribs with dimples, V-pattern ribs with a combination of grooves, W-ribs, and V-discrete ribs). Creation of flow separation areas has the greatest influence on the flow behavior of a rib. This recirculation/vortex flow accounts for turbulence, which promotes both heat transfer and pressure losses. More specifically, it has been shown that perforations in ribs and V-shaped ribs can improve thermal performance and minimize pressure losses.

5. Enhancing heat transfer with baffles

For heat transfer in compact heat exchangers, ultra-baffles are needed that are appropriate for the sizes of the heat exchangers. Baffles of several designs have been proposed.

5.1 Effect of transverse baffles

Heat transfer and flow structure in a channel with inline baffles have been predicted numerically by Bazdid-Tehrani and Naderi-Abadi [65]. They claimed that baffles with high blockage ratios were ineffective in improving heat transfer. Oils were used as the working fluids in Mousavi and Hooman [66] investigated the influence of segmented baffles on the top and bottom channel walls to improve heat transfer rate. Chang et al. [67] examined at how oblique baffles affected thermal performance. They claimed that the baffles significantly improved the rates of heat transfer and pressure loss over those determined by the Dittus-Boelter and Blasius correlations. Additionally, the maximum thermal performance reached 3.4. Al_2O_3/water nanofluid heat transfer behaviors were investigated in experiments by Mashaei et al. [68] in a channel with baffles. Development of the nanofluid flow induced an increased intensity and reduced length of the recirculation regions over those found using water alone.

5.2 Effect of inclined baffles

Promvonge et al. [69, 70] evaluated the effect of installing 45° angled baffles in a duct on its heat transfer. They noticed that pressure drop and heat transfer rose as baffle height increased. When the channel height is 20% and the baffle is at a 45° angle, the thermal enhancement is greatest. Kwankaomeng and Promvonge [71] examined the thermal characteristics of a channel with inclined baffles. They discovered that the tvortex flow produced by a baffle preferred to cause impinging flows, which greatly boosted heat transfer throughout the channel. The greatest Nusselt number ratio and thermal performance were identified to be 7.9 and 3.1, respectively. Promvonge et al. [72] analyzed thermal behavior and fluid flow in a channel with inclined baffles on the top and bottom walls. They exhibited P-vortex flows and that the inter-baffle cavity walls substantially boost thermal enhancement.

5.3 Effect of perforated baffles

Perforated baffles can create jets impinging on exchanger surfaces to improve heat transfer. Additionally, the presence of holes also helps in reducing pressure losses. This results in better thermal performance. The report by Dutta et al. [73], shows that installing perforated baffles improves heat transfer by up to 5 times compared to that of a bare channel. Moreover, the jets introduced by perforated ribs promote a greater degree of heat transfer than the common secondary flow provided by non-perforated ribs [74]. Sahel et al. [75] measured the thermal performance of a channel with fitted perforated baffles. They revealed that perforated baffles with pore axis ratios of 0.19 produced approximately 65% greater heat transfer thantraditional baffles. El Habet et al. [76] examined the impact of baffle perforation ratios and tilt angles (as seen in Fig. 37) on heat transfer rate and thermal performance. The highest thermal performance was achieved at a tilt angle of 60° and a perforation ratio of 10%.
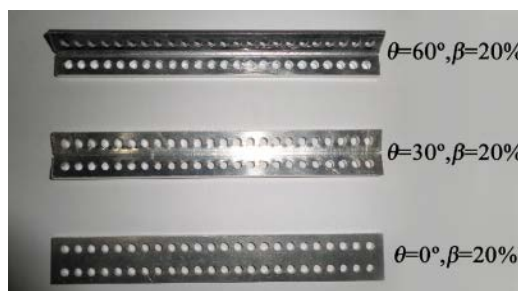

Fig. 37. Transverse and V-shaped ribs [76].

Baffle perforation ratios (10–40%) and tilt angles (0°, 30°, 45°, and 60°) were studied by El Habet *et al.* [76], examining their effects on heat transfer, pressure losses, and thermal performance. At a perforation ratio of 10% and a tilt angle of 60°, the maximum thermal perfromance was achieved. According to Alam *et al.* [77], compared to a conventional V-shaped baffle, perforated V-shaped baffles (Figs. 38–40) could boost heat transfer and thermal enhancement while decreasing pressure losses. Chamoli [78] and Chamoli and Thakur [79, 80] investigated numerically the geometry of V-down shaped perforated baffles in order to obtain minimal pressure losses and maximum heat transfer. According to them, the maximum Nusselt number and pressure losses were obtained at a 12% open area. Promvonge and Skullong [81] studied the thermal performance of a duct with V-shaped flapped baffles with a chamfered groove, depicted in Fig. 41. According to their findings, baffles with a tilt angle of 90° had the lowest heat transfer because they produced the least powerful counter-rotating vortices among those of four flap angles (30°, 45°, 60°, and 90°) placed in the central area of the baffle.
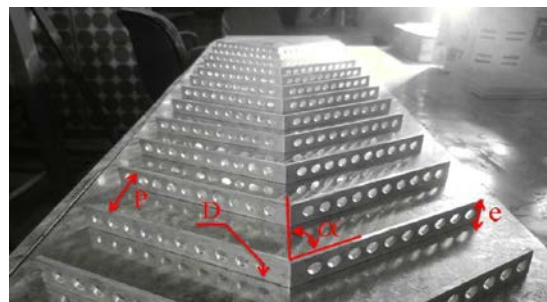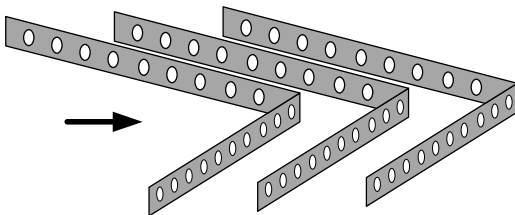

Fig. 38. Perforated V-shaped baffles [77].
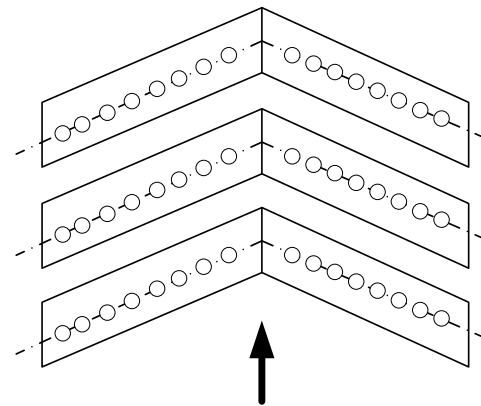

Fig. 39. V-down shaped perforated baffles [78].
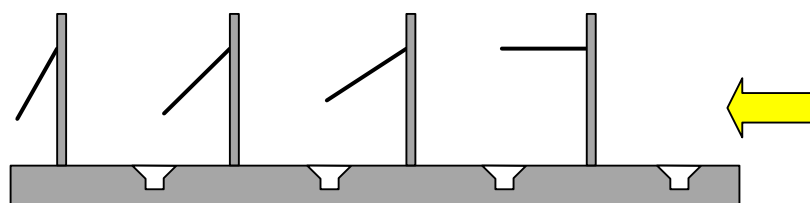

Fig. 40. V-down shaped perforated baffles [79].

Fig. 41. V-shaped flapped baffles combined with chamfered groove [81].

5.4 Effect of V-shaped baffles

Generally, V-shaped ribs induce axial vortices after impact with the ribs. Such a change in flow characteristics will cause collision of low temperature fluid with both the upper and lower walls, improving fluid mixing and heat transfer. The results of Eiamsa-ard *et al.* [82] reveal that each pair of thin V-shaped ribs induces four longitudinal vortices. Two are induced by the top rib and the other two by the bottom one. The vortices assist in the transfer of heat from a heated surface to the fluid (Figure 42). The illustration also shows that slender V-shaped ribs with an angle of attack of 45° are more effective at enhancing heat transfer than those with attack of 60°, as indicated by a thinner high temperature layer (red layer).

(a) $\alpha = 45^{\circ}$ at $Re = 1000$ and $BR = 0.15$

(b) $\alpha = 60^{\circ}$ at $Re = 1000$ and $BR = 0.15$
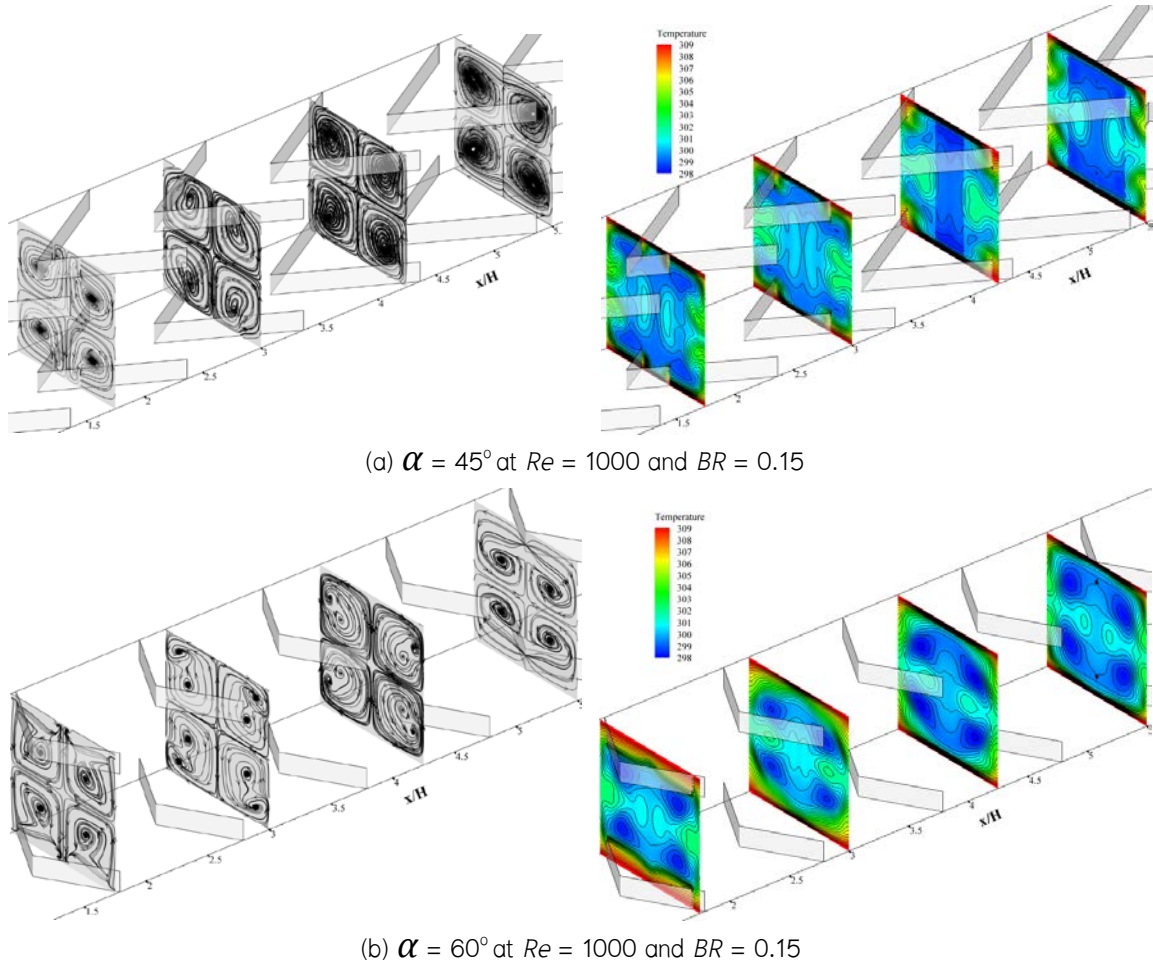
Fig. 42. Axial vortex flows on the vertical planes and temperature distributions on the vertical planes in a square channel equipped with thin V-shaped ribs [82].

Fig. 43 shows that V-shaped ribs with $\alpha = 45^{\circ}$ introduce reattachment flow that covers a larger area than those having $\alpha = 60^{\circ}$. The ribs at $\alpha = 45^{\circ}$ distribute reattached flow from the whole bodies of the ribs while the ones with $\alpha = 60^{\circ}$ cause reattahment only around the rib center. The 3D iso-surface flow patterns in Fig. 44 support the observation that the V-shaped ribs with $\alpha = 45^{\circ}$ introduce vortices with higher strength (observed from the larger ring diameter) than the ones with $\alpha = 60^{\circ}$. Fig. 45 confirms that V-shaped ribs with $\alpha = 45^{\circ}$ provide a high Nusselt number area closer the the rib rear with higher intensity than the ones with $\alpha = 60^{\circ}$, as shown in Figs. 42-44.

(a) $\alpha = 45°$ (b) $\alpha = 60°$

Fig. 43. Discharge current line from V-shaped ribs at $Re = 1000$ and $BR = 0.15$ [82].

(a) $\alpha = 45°$ (b) $\alpha = 60°$
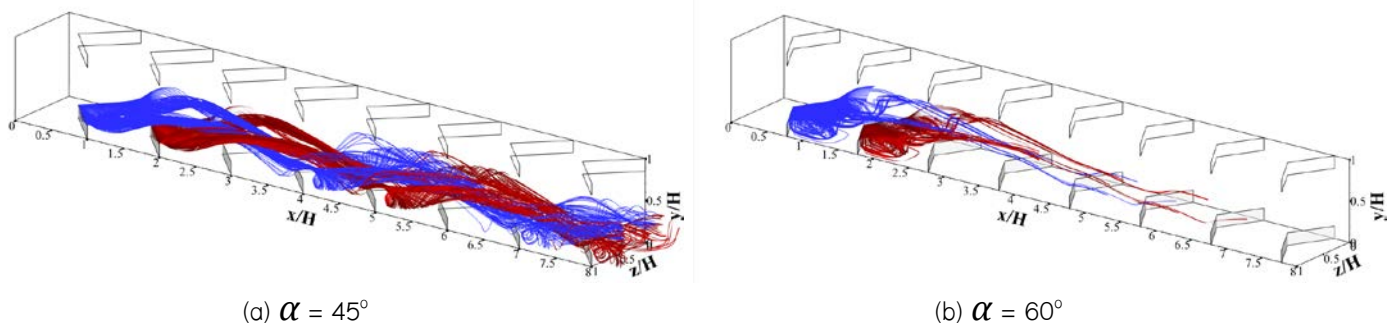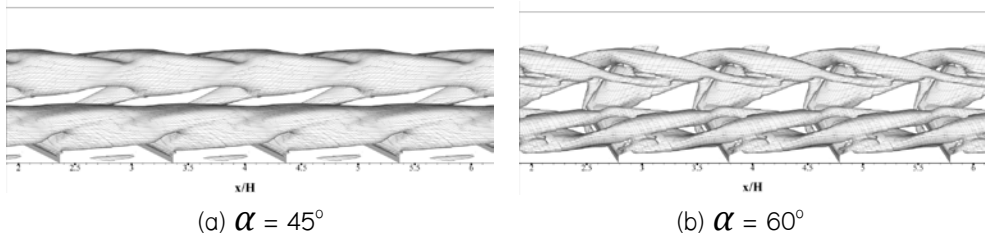
Fig. 44. The 3D surface flow (iso-surface) introduced by V-shaped ribs at $Re = 1000$ and $BR = 0.15$ [82].

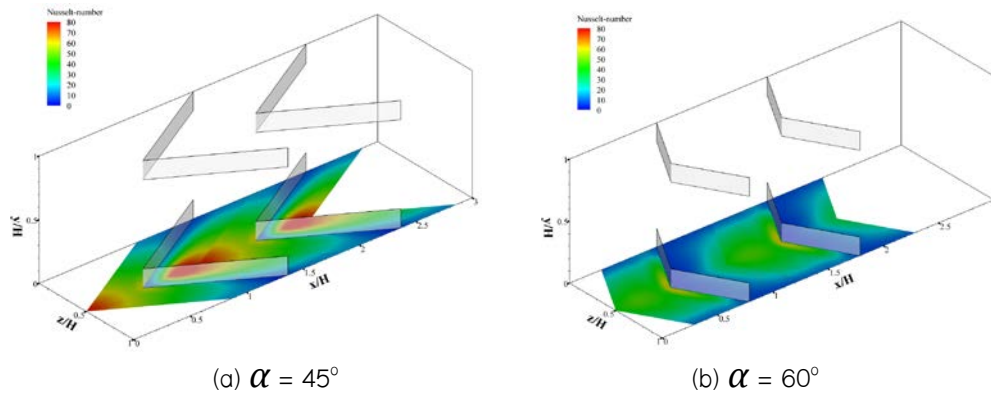(a) $\alpha = 45°$ (b) $\alpha = 60°$

Fig. 45. Nusselt number contours yielded by V-shaped ribs at $Re = 1000$ and $BR = 0.15$ [82].

Multiple v-shaped ribs, including the V/W-shaped rib, the multi V-shaped rib, the arch-shaped rib, the broken V-shaped rib, the broken multi V-shaped rib, and double V baffles, are illustrated in Figs. 46 to 61. These ribs are intended to boost the heat transfer rate. In accordance to research by Abraham and Vedula [61], Thakur *et al.* [83], Li *et al.* [84], and Jiang *et al.* [85], angled ribs (V- and W-shaped ribs) were able to generate counter-rotating flows and provided better heat transfer than transverse ribs (Fig. 46). Abraham and Vedula [61] found that the V-shaped arrangement offered the greatest performance. A study by Thakur *et al.* [83] and Li *et al.* [84], V- and W-shaped ribs give a greater rate of heat transfer than inclined ribs (Figures 47–49). Tanda and Satta [86] noticed that angled ribs generate a vortex flow that helps reduce wall temperature and improve heat transfer. Jin *et al.* [87, 88] and Li *et al.* [89] revealed that the arrangement of multiple V-shaped ribs (Figs. 50–51) on one wall of a solar air radiator generated a pair of counter-rotating vortices. The V-shaped ribs (Fig. 49) placed on the upper and lower walls produced four counter-rotating vortices, as reported by Fawaz *et al.* [90] and Bahiraei *et al.* [37]. This flow structure's disruption of a thermal boundary layer and increased heat transfer at the jet's impinged surface improved thermal performance. In the work of Ebrahim Momin *et al.* [39], V-shaped ribs with a higher rib height caused increased pressure losses

and heat transfer. Dong *et al.* [91] used solar air heater with inclined groove rolling surfaces. They noted that as the number of rolling surfaces (*N*) increased, the number of counter-rotating flows on the transverse plane also boosted resulting in enhanced fluid interaction resulting in heat transfer. Singh *et al.* [92] discovered that raising the number of arc-shaped ribs increased the heat transfer rate and friction factor by as much as 5.07 and 3.71 times, respectively, compared to a plain channel. Angled baffles and ribs have been altered in a variety of ways, including adding discrete/broken perforations. This was done to improve the thermal performance factor. Discrete V-down ribs offer lower pressure losses and greater heat transfer than the continuous V-down ribs, according to Singh *et al.* [93, 94], who investigated the effects of discrete baffles/ribs. According to Kumar *et al.* [95], disruption of the boundary layer by air passing through a gap increased heat transfer behind the rib. Furthermore, it was claimed that powerful secondary stream jets were produced by broken multiple V-type baffles (in the form of counter-rotating vortices). Maithani and Saini [96] also indicated that broken V-type baffles with small gaps provided the greatest heat transfer. Kumar *et al.* [97] analyzed the thermal performance and optimal relative width parameter of the channel using multiple broken V-shaped baffles. According to their findings, a relative baffle width of 5.0 resulted in superior thermal performance overall. In addition, the results suggested that the thermal performance of the broken multiple V-type baffles was more beneficial to that of the other baffles.
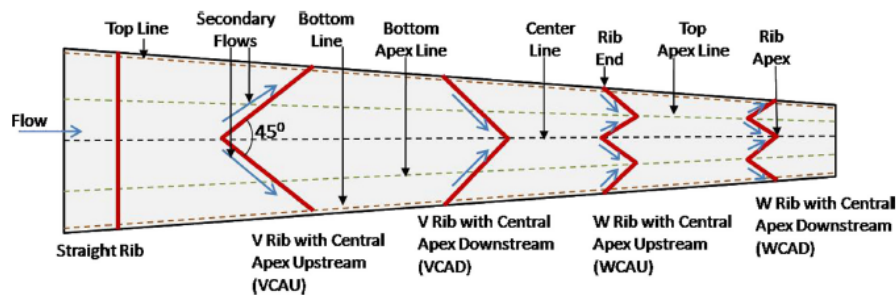
Fig. 46. V- and W-shaped ribs [61].

Fig. 47. V-shaped ribs [83].

Fig. 48. W-shaped ribs [84].
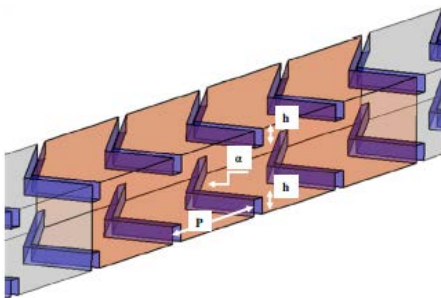

Fig. 49. Multi V-shaped ribs [90].

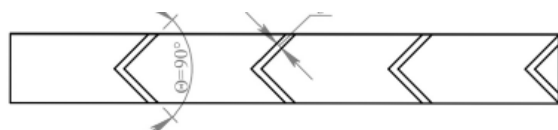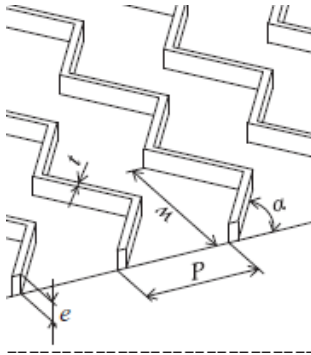**Fig. 50.** V-shaped ribs [37].

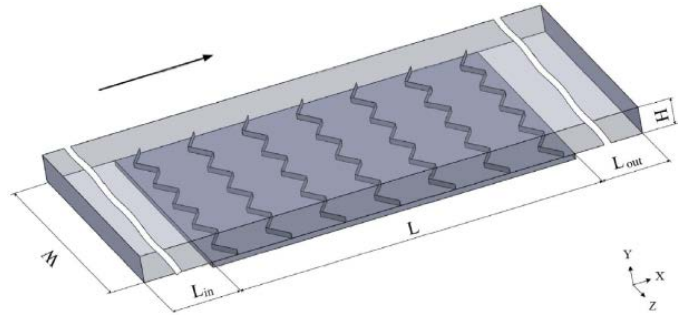**Fig. 51.** Multi V-shaped ribs [88].

Fig. 52. Multi V-shaped ribs [89].
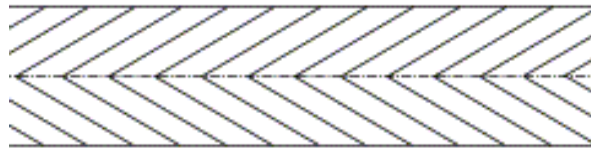

Fig. 53. V-shaped ribs with the greater rib height [39].
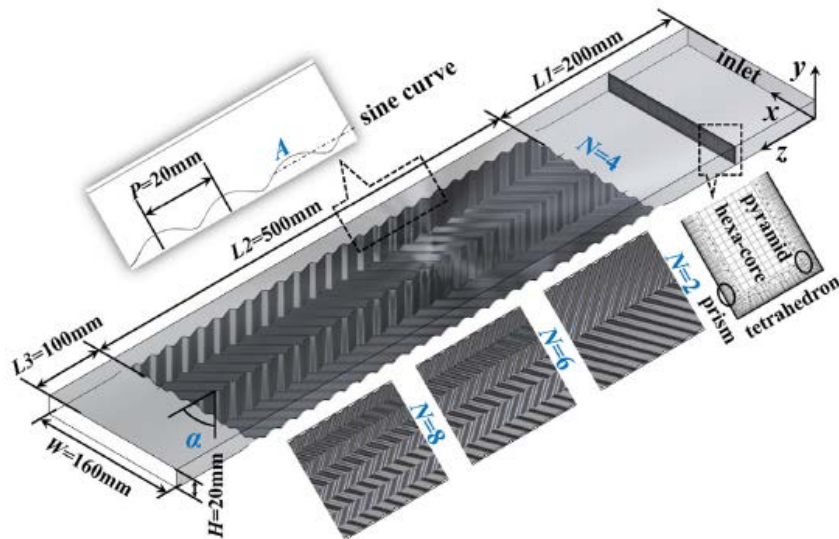

Fig. 54. Inclined groove ripple surfaces [91].

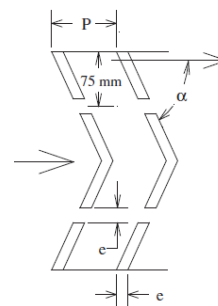**Fig. 55.** Arc-shaped ribs [92].

Fig. 56. Continuous V-down ribs [93].
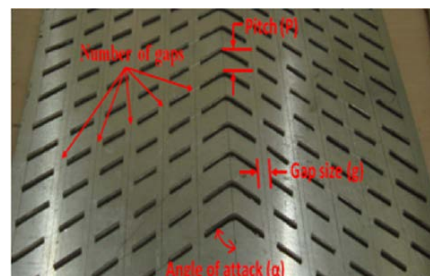
Fig. 57. Broken V−type baffles [96].

Fig. 58. Broken multiple V−type baffles [97].

Jedsadaratanachai and Boonloi [98] examined how a channel with 30° double V−baffles (Fig. 69) might improve heat transfer rate. They studied how various blockage ratios (0.05−0.25) and pitch ratios (1.0−2.0) affected thermal performance. It was found that increasing the blockage ratio while reducing the pitch ratio led to rose pressure losses and heat transfer. The greatest thermal performance, 3.2, was found at blockage and pitch ratios of 0.1 and 1.0. Jedsadaratanachai and Boonloi [99] examined the performance of a duct with hybrid discrete baffles or V−baffle/orifice (Fig. 60), examining the heat transfer, pressure losses, and thermal performance in the turbulent flow regime. At a blockage ratio of 0.1, the baffles boosted the heat transfer rate and thermal performance by up to 6.0 and 1.7 times, respectively. A variety of V−type baffles with 60° splits and various width ratios (Fig. 61) were presented by Kumar et al. [97]. According to their research, broken multiple V−type baffles surpassed other baffles in terms of thermal performance. Kumar et al. [100] utilized discretized broken V−pattern baffles with attack angles of 30−70°, blockage ratios of 0.25−0.8, pitch ratios of 0.5−2.5, and baffle gap width ratios of 0.5−1.5 to improve heat transfer. The discretized broken V−pattern baffle gave better than other baffles in terms of thermal performance. The heat transfer behaviors of a channel with discretized broken V−pattern baffles with different baffle gap ratios (0.26 to 0.83) and baffle gap width ratios were also tested by Kumar et al. [101]. The greatest thermal performance was 3.14. Fawaz et al. [90] determined flow topology and heat transfer mechanisms in a duct with V−baffles inserted at a 45° attack angle with varying blockage (0.2−0.6) and pitch ratios (0.5−1.5). They predicted that the four counter−rotating vortices produced by the V−baffle would result in chaotic mixing between the wall and core flow areas. Promvonge and Skullong [102] proposed straight tapes with double−sided V−baffles installed with various blockage and pitch ratios for enhanced heat transfer. In their experiments, the tapes were arranged in two different configurations, with the V−apex pointing upstream and downstream. The ones with the V−apex pointing upstream underperformed the ones with the V−apex pointing downstream by about 1.4%. The greatest thermal performance factor, 2.07, was attained at a blockage ratio of 0.15 and a pitch ratio of 1.0. Promvonge and Skullong did research on newly redesigned V−shaped baffles [103]. While the blockage and pitch ratios were varied between 0.1−0.2 and 0.5−2.0, respectively, the attack angle of the baffles remained constant at 30°. Modified V−shaped baffles with a blockage ratio of 0.15 and a pitch ratio of 0.1 had thermal performance factors of up to 2.34. Promvonge and Skullong [81] examined the thermal performance of a channel with a coupled V−shaped flapped−baffle and chamfered−groove, four different flap angles installed on the central region of the baffle (30°, 45°, 60°, and 90°), a baffle pitch ratio of 1.0−2.0, and a groove pitch ratio of 1.0−2.0. The ideal baffle design had a 1.5 pitch ratio and a 45° flap angle placed in the baffle center region, yielding a high thermal performance factor, 2.68.
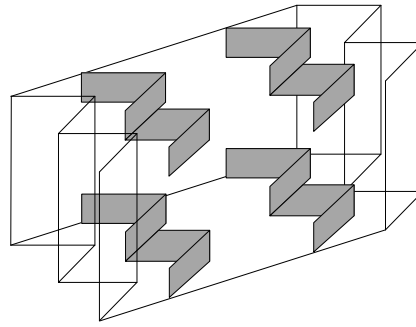
Fig. 59. 30° double V–baffles [98].
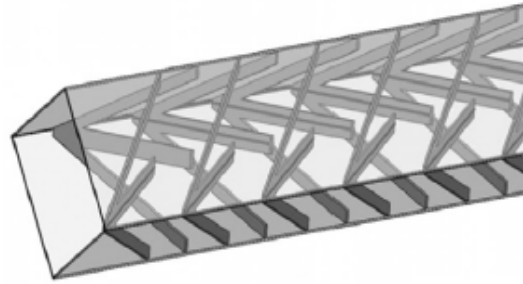
Fig. 60. Discrete Combined V–baffle and V–orifice [99].

Fig. 61. Broken Multiple V–type baffle [97].

5.5 Effect of broken V–shaped baffles

Segregated V–shaped baffles can generate secondary vortex flows as well as longitudinal vortex flows. The results by Promvonge *et al.* [36] reveal velocity, temperature and pressure fields as well as Nusselt number contours associated with the use of segregated V–shaped baffles (Fig. 62). Clearly, counter longitudinal eddy currents appear at the lower wall near each V–shaped rib. Low pressure at the rib rear induces fluid movement from the main flow down to the hot wall. Then, the fluid moves upward with transferred heat. The process is continuously repeated at each rib. Since baffles have smaller pitch ratios (*PR*) than square ribs, they therefore show different heat transfer behaviors, as depicted in Fig. 63. This figure suggests that the density and intensity of eddy currents and Nusselt numbers for baffles, are greater than square ribs, owing to their smaller pitch ratio. Consequently, heat transfer with baffles is superior to that of the square baffles, especially around the middle of the channel and in front of the ribs. However, heat transfer along lateral region by the baffles is slightly lower than that of square baffles. Kumar *et al.* [101] evaluated the heat transfer rates in a channel with discretized broken V baffles installed. Thermal performance indices reaching 3.14 with up to 4.47 times greater heat transfer were seen over that of a smooth channel. The thermal performance of a solar air heater with multiple broken V–shaped baffles installed was compared to those of a channel with conventional baffles by

Kumar *et al.* [97]. According to their findings, broken multiple V–shaped baffles outperformed conventional baffles in terms of thermal performance.
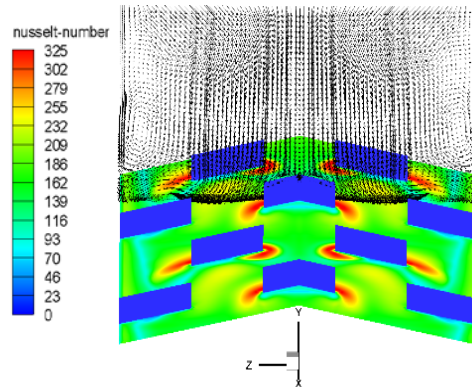
(a) Fluid velocity field and surface Nusselt number contour
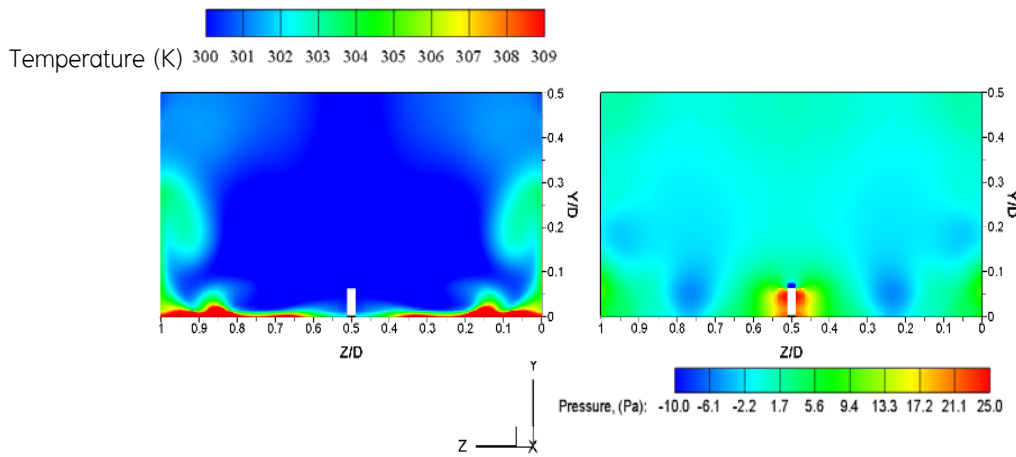
(b) Temperature and pressure fields

Fig. 62. Velocity field, surface Nusselt number contour, temperature and pressure fields in the channel with segregated V–shaped baffle at *BR* = 0.0625, *PR* = 0.625 and *Re* = 15,000 [36].
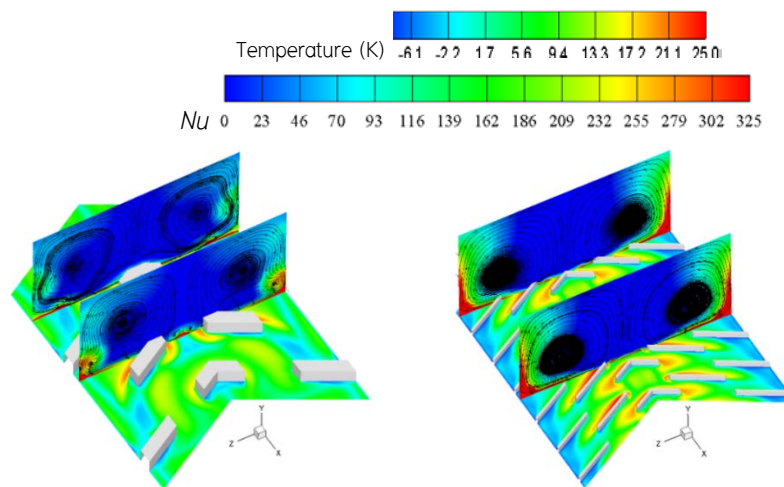
(a) square rib PR = 0.6250, BR = 0.0625   (b) PR = 0.1875, BR = 0.0250

Fig. 63. Perpendicular flow lines in each cross–section and contour of the Nusselt numbers on the surface at *Re* = 15,000 and α = 60° [36].

5.6 Effect of twisted baffles

Two types of twisted ribs [104] have been proposed for application in a ribbed channel. They are typical twisted ribs and an alternating axis twisted ribs, as depicted in Fig. 64. Flow patterns and Nusselt number contours associated with the application of typical thin and common/alternating axis twisted baffles are display in Figs. 65 and 66, respectively. The fluid flow across a typical baffle shows common reattachment, while that across the common/alternating axis twisted baffles (Fig. 66) is slightly diffracted, leading to spiral flow prior to reattachment. Subsequently, the Nusselt number on the wall surface varies. However, the mean Nusselt numbers in all cases are comparable. Among all ribs, a typical baffle has the highest friction losses. Both common twisted ribs and alternating axis twisted baffles cause comparable friction losses, which are lower than for a typical baffle. This arises because common twisted baffles and alternating axis twisted baffles facilitate fluid flow in a spiral pattern. Therefore, twisted baffles show promising potential in promoting thermal performance. Eiamsa–ard [105] investigated how multiple twisted tapes improved heat transfer in a duct. He looked at the influences of free–spacing ratios and tape twist ratios. According to experimental findings, a channel with multiple twisted tapes could transfer heat up to 167% more efficiently than a smooth channel. As free–spacing ratio and tape twist ratio decreased, heat transfer and pressure losses increased. The thermal performance of a solar air heater equipped with twisted ribs was investigated by Kumar and Layek [106–107]. The effects of pitch ratio (p/e), rib inclination angle (30°–90°), and twist ratio (y/e = 3.0–7.0) were examined. When twisted rib turbulators (Fig. 67) were utilized, heat transfer and pressure drop increased up to 2.58 and 1.78 times, respectively, compared to a plain channel. Rashidi *et al.* [108] revealed the thermal performance of a square duct attached with transverse twisted baffles. The baffle with a pitch intensity of 540° resulted in the lowest pressure losses, whereas the baffle with a pitch intensity of 360° had the maximum heat transfer. Thermal enhancement was studied by Eiamsa–ard and Chuwattanakul [17] in a channel with inclined twisted–baffles (Fig. 68), different pitch ratios and baffle twist ratios. The highest thermal performance factors, up to 1.98, were provided by inclined twisted–baffles (p/w = 6.0 and y/w = 5.0). The thermal performance factor produced by the improved channel reached 1.98. The thermal performance of a micro/mini–channel heat sink with twisted ribs installed was studied by Zhang *et al.* [109]. Their results demonstrated that twisted or inclined ribs in mini–channels simultaneously improved both flow resistance and heat transfer. Thermal efficiency was enhanced by increasing the twist angle and decreasing the height of the twisted ribs. The micro/mini–channel heat sink with twisted ribs had an overall maximum thermal performance factor of 1.34. According to Sawhney *et al.* [110], heat transfer from wavy delta winglets (Fig. 69) was about 223% higher than that for a smooth channel.

Fig. 64. Twisted baffles [104].

(a) Transverse baffles   (b) Alternate axis twisted baffles
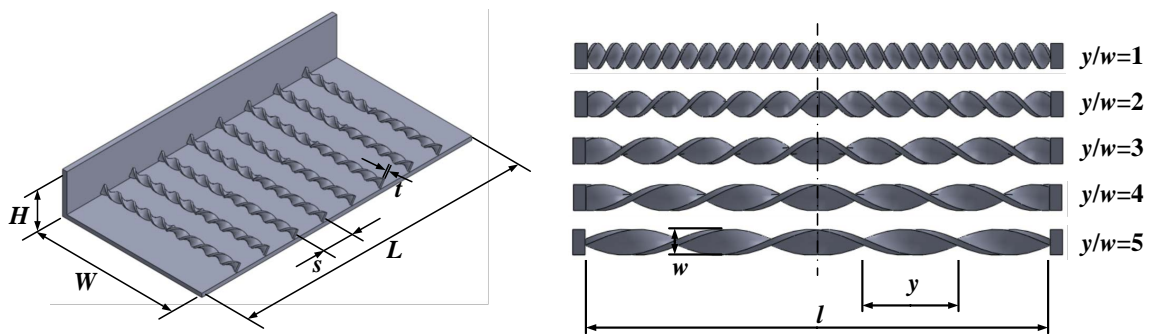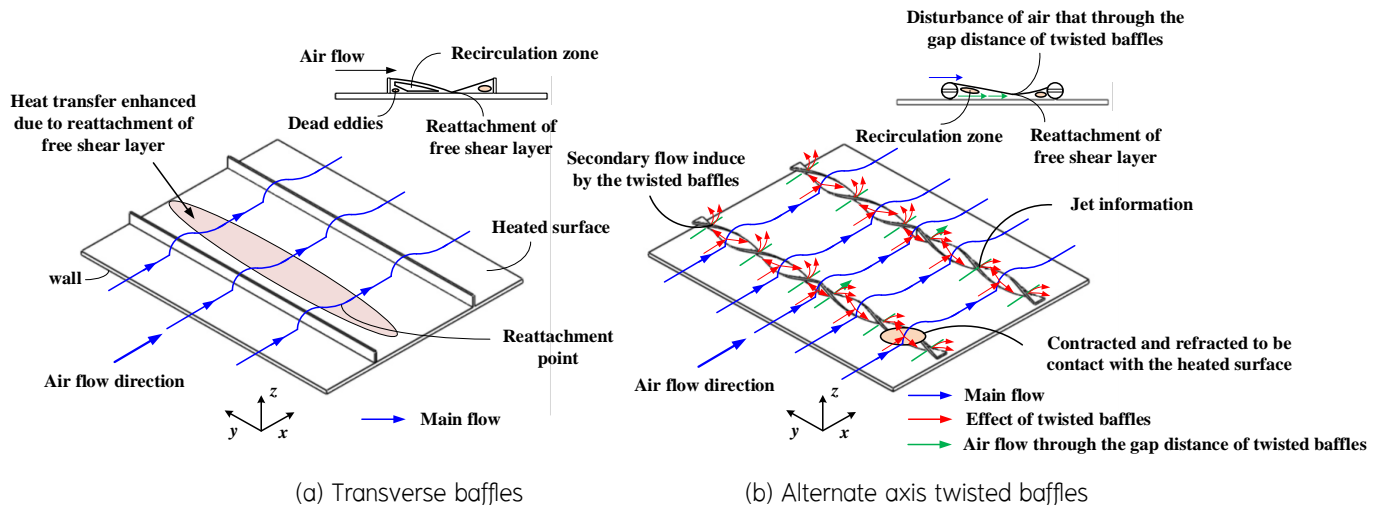
Fig. 65. Flow patterns through transverse baffles and alternate axis twisted baffles [104].

(a) Transverse baffles   (b) Alternate axis twisted baffles
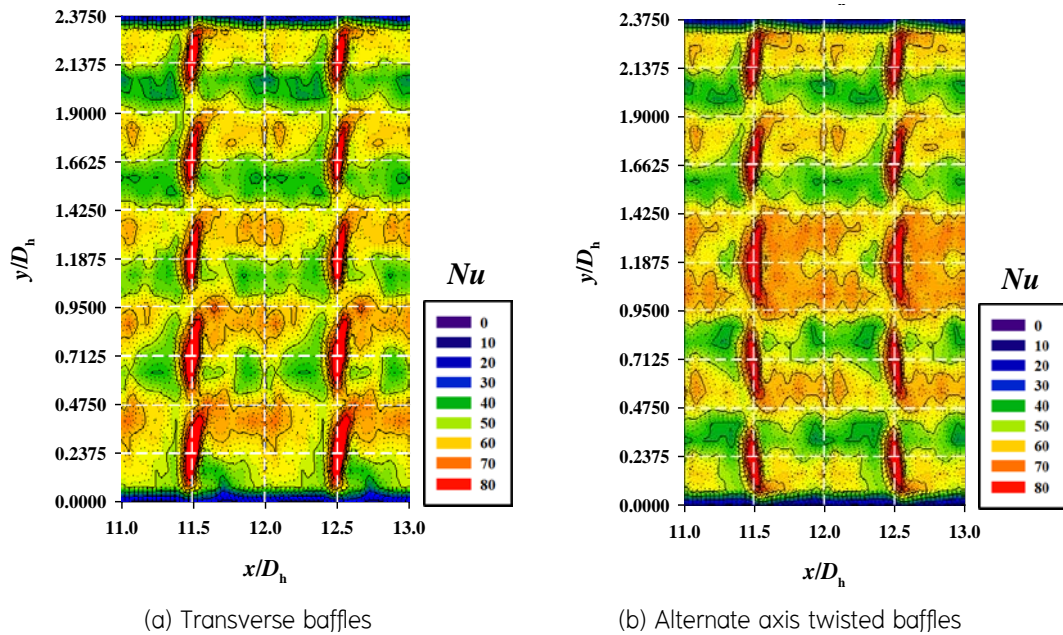
Fig. 66. Nusselt number distributions in the channels installed with a typical baffle, common twisted rib and alternating axis twisted ribs at a Reynolds number of 9000 [104].

Fig. 67. Twisted ribs [106–107].
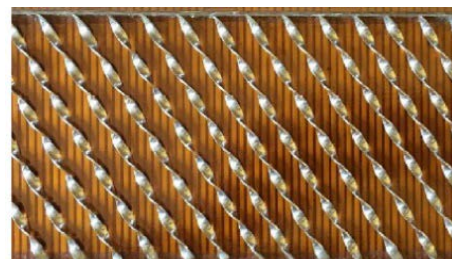
Fig. 68. Inclined twisted–baffles [17].
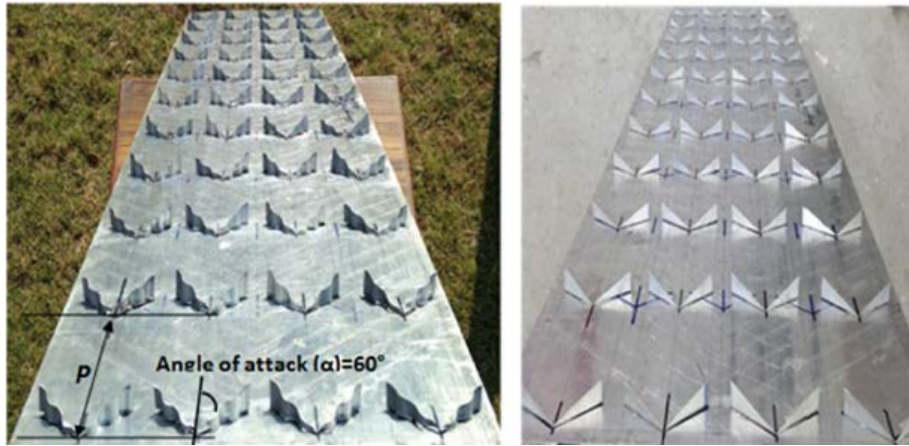
Fig. 69. Wavy delta winglets Sawhney *et al.* [110].

5.7 Effect of arc-shaped wires/ribs/ baffle

Sahu and Prasad [111] evaluated the thermal performance of a channel with a fitted roughened arc-shaped wire (Fig. 70). It was discovered that a pitch ratio of 10, blockage ratio of 0.0422, and relative attack angle of 0.3333 produced the greatest flow reattachment and separation regions. In comparison to a conventional channel, the exergetic efficiency increased by up to 56%. Hans *et al.* [112] examined a solar heater fitted with broken arc-ribs (Fig. 71). They were able to reach heat transfer rates and pressure drop that were 1.19 and 1.14 times higher, respectively, than those of an arc-ribbed channel and a plain channel. Secondary flows brought on by broken arcs were the cause of this. Saravanakumar *et al.* [113] used analytical modeling to investigate the effects on the thermal performance of a channel with arc-shaped ribs installed. They discovered that arc-shaped ribs (Fig. 72) installed at width of the baffle and length of the baffle of 0.015 m and 0.2 m performed the greatest enhancement in thermal performance, to 82%, an increase of 28%. The influences of arc-shaped baffles (Fig. 73) on thermal performance were investigated by Promvonge *et al.* [114]. They revealed that the heat transfer was as great as 5.8%, 3.9%, 2.3%, and 2.5% higher at an attack angle of 90° than it was at 20°, 40°, 60°, and 80°, respectively. To achieve the highest thermal performance factor, 1.43, arc-shaped baffles with an angle of 90° and an 8.0 pitch ratio were used. Sureandhar *et al.* [115] evaluated the thermal performance, effectiveness of a channel fitted with arc-ribbed wire. An optimal 50% thermal performance was determined. As the volumetric airflow grew, the overall loss coefficient was reduced while the efficiency rose.
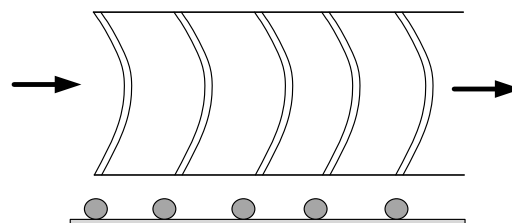
Fig. 70. Arc shape wire roughness [111].

Fig. 71. Broken arc rib [112].
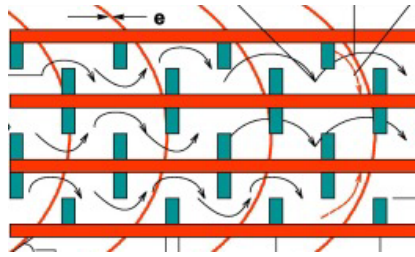
Fig. 72. Arc shaped rib [113].
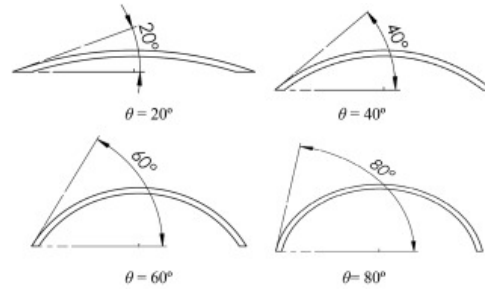
Fig. 73. Arc-shaped baffle [114].

5.8 Summary of baffles

It is efficient to use baffles to improve the thermal performance of heat exchangers and solar air purifiers. Numerous researchers have investigated the effect of these dividers on heat transfer rate and pressure loss characteristics in air ducts. Perforations in baffles, V-shaped baffles, and twisted baffles have the potential to enhance thermal performance and reduce pressure losses, as discussed in the preceding sections.

6. Combined enhancement device

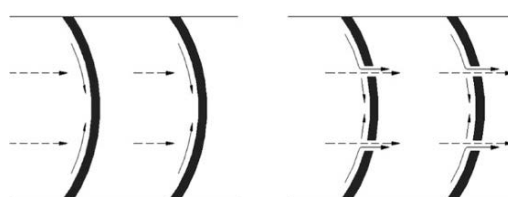Recently, combined enhancement devices with roughened surfaces were used as vortex generators in a solar air heater duct. In a channel, Promvonge *et al.* [116] examined the influences of ribs and winglet-type on heat transfer and pressure loss characteristics. To create longitudinal vortex flows in the test duct, two sets of winglet-type devices with different attack angles were mounted at the channel's inlet, isosceles triangular-shaped ribs were installed inside duct walls to create a reverse flow. Their results demonstrate that combined enhancement devices, ribs and winglet-type, produced increased heat transfer over that of individual enhancement devices (rib). Furthermore, it was found that WVGs with higher attack angles were better at transferring heat. Promvonge *et al.* [117] additionally examined at the way inserting ribs and delta-winglets (DWs) together improved heat transfer in a solar air heater. With ribs, a DW that is pointed upstream (PU-DW) is more effective at transferring heat than a DW that is pointed down (PD-DW). The DW with the smallest attack angle and pointing downstream provided the greatest thermal performance.

7. Nano-fluid heat transfer enhancement

As novel liquids, nanofluids are finding new applications in heat exchangers [118-120]. Nanoparticles are particles with sizes less than 100 nanometers (nm). Poor thermal conductivity of a basic fluid necessitates the utilize of nanoparticles to improve heat transfer efficiency. The concept is to enhance the heat transfer capacity of a material by increasing its thermal conductivity. This is done by including solid particles with higher heat conductivity than the original fluid. Compared to the thermal conductivity of the base fluid, a metal-specific solid is hundreds of times better. Nonetheless, advancements in nanofluids technology are still required. The limitations of current technology mean that the nanofluids and nanoparticles used in their synthesis are expensive, and that only a small amount can be produced at a time. Additionally, most nano-fluids become unstable after prolonged use, a problem that is addressed by adding other chemicals to the working fluid.

8. Summary

This review concludes that a significant portion of study has been performed on the influence of artificial roughness of geometries shapes and conditions on flow structure, heat transfer rate and pressure loss characteristics. A considerable improvement in heat transfer rate can be accomplished with little increase in pressure losses. As a result, further conclusions can be drawn.

1. The thermal performance of solar air heaters is often worse that of solar water heaters due to the absorber plate's naturally weak heat transfer capabilities with the air passing through a duct. Heat transfer coefficient improvements are needed to make commercialization of solar air heaters possible. Improving the air-to-absorber plate convective heat transfer coefficient (h) may be done in two primary ways. The first technique involves increasing the area of heat transfer by employing corrugated surfaces or enlarged surfaces known as fins, without affecting the convective heat transfer coefficient (h). The second way of boosting convective heat transfer by generating surface disturbances. That can be implemented using ribs/baffles the bottom of the absorber surface. Several researchers have sought to create ribs/baffles that may improve the coefficient of convective heat transfer (h) with negligible pressure losses.

2. Modified rib/baffle designs have been explored to promote an important heat transfer gain, over that of a plain channel, for the simplest ribs and baffles for solar air heaters and for gas turbines. The redesigned ribs/baffles have a positive influence on efficiency by reducing the pressure loss, which in turn reduces pumping power and so saves energy.

3. There are numerous designs of ribs and baffles. Well-designed ribs and baffles efficiently augment heat transfer while keeping pressure loss as low as possible to maximize the thermal performance factor. A thermal performance factor above unity indicates that an enhanced system is promising for energy saving.

4. Recent studies show that newly designed baffles improve thermal performance by boosting heat transfer rate while minimally increasing pressure drop. According to a review of baffles, perforations are an excellent way to minimizing pressure loss without significantly reducing the heat transfer rate. Perforated baffles present higher thermal performance compared to solid baffles.

5. Development of ribs and baffles focuses on varying their shape, geometry and arrangement. Flows through the ribs and baffles are extremely complex. Without an experimental study, numerical investigation allows a deeper understanding of flow and heat transfer mechanisms associated with enhanced systems. The advantages of numerical methods are that they allow researchers to examine issues that cannot be practically studied by experimentation. They also allow deeper research for investigating whether two or more variables are related. Understanding flow and thermal behaviors is essential for the continued development of ribs and baffles that improve heat transfer.

References

[1]   Han JC, Chandra PR, Lau SC. Local heat/mass transfer distributions around sharp 180 deg turns in two-pass smooth and rib-roughened channels. J Heat Transf. 1988;110(1):91-98.

[2]   Nikuradse J. Laws of flow in rough pipes. National Advisory Committee for Aeronautics; 1950.

[3]   Varun, Saini RP, Singal SK. A review on roughness geometry used in solar air heaters. Sol Energy. 2007;81(11):1340-1350.

[4]   Webb RL, Haman LL, Hui TS. Enhanced channels in electric utility steam condensers. Heat transfer in Heat Rejection Systems – ASME Symposium. 1984;37(2):17-26.

[5]   Bergles AE. Techniques to enhance heat transfer. In: Rohsenow WM, Hartnett JP, Cho YI, editors. Handbook of Heat Transfer. 3rd ed. New York: McGraw-Hill; 1998.

[6]   Manglik RM. Heat transfer enhancement. In: Bejan A, Kraus AD, editors. Heat Transfer Handbook. New Jersey: Wiley; 2003.

[7]   Webb RL, Kim NK. Principles of Enhanced Heat Transfer. Florida: Taylor & Francis; 2005.

[8]   Zimparov VD, Vulchanov, N. Performance evaluation criteria for enhanced heat transfer surfaces. Int J Heat Mass Transf. 1994;37(12):1807-1816.

[9]   Webb RL, Bergles AE. Performance evaluation criteria for selection of heat transfer surface geometries used in low Reynolds number heat exchangers. Washington DC: Hemisphere; 1983.

[10]   Wang L, Sundén B. Performance comparison of some tube inserts. Int Commun Heat Mass Transf. 2002;29(1):45-56.

[11]   Webb RL, Kim NH. Principle of Enhanced Heat Transfer. New York: Taylor & Francis; 1994.

[12]   Zhang G, Sundén B, Xie G. Combined experimental and numerical investigations on heat transfer augmentation in truncated ribbed channels designed by adopting fractal theory. Int Commun Heat Mass Transf. 2021;121:105080.

[13]   Ke Z, Zhang Y. Heat transfer enhancement in a rectangular channel with flow-induced pitching, heaving or surging of an airfoil. Int Commun Heat Mass Transf. 2023;142:106657.

[14]   Zhao Z, Luo L, Du W, Wang S, Zhou X, Sundén B. Experimental study on the augmented Nusselt number of the endwall through a square-sectioned sharp-turn channel using novel heat exchanger. Int J Heat Mass Transf. 2022;192(15):122920.

[15]   Eiamsa-ard S, Sripattanapipat S, Promvonge P. An experimental study of a channel flow over two obstacles hydrogen bubble technique. 7th Asian Symposium on Visualization; 2003 Nov 3-7; National University of Singapore, Singapore: ASV; 2003. p. 3A-1.

[16]   Eiamsa-ard S, Changcharoe, W. Analysis of turbulent heat transfer and fluid flow in channels with various ribbed internal surfaces. J Therm Sci. 2011;20:260-267.

[17]   Eiamsa-ard S, Chuwattanakul V. Visualization of heat transfer characteristics using thermochromic liquid crystal temperature measurements in channels with inclined and transverse twisted-baffles. Int. J Therm Sci. 2020;153:106358.

[18]   Yongsiri K, Eiamsa-ard P, Wongcharee K, Eiamsa-ard S. Augmented heat transfer in a turbulent channel flow with inclined detached ribs. Case Stud Therm Eng. 2014;3:1-10.

[19]   Sripattanapipat S, Eiamsa-ard S, Kongkaitpaiboon V, Promvonge P. Forced convection heat transfer and flow characteristics in a rectangular channel with 90o baffles. Proceedings of 12th Asian Symposium on Visualization; 2013 May 19-23; Tainan, Taiwan: ASV; 2013. p.XX-XX.

[20]   Nuntadusit C, Wae-hayee M, Bunyajitradulya A, Eiamsa-ard S. Thermal visualization on surface with a transverse perforated rib. Int Commun Heat Mass Transf. 2012;39(5):634-639.

[21]   Changcharoen W, Eiamsa-ard S. Numerical investigation of turbulent heat transfer in channels with detached rib-arrays. Heat Transf. 2011;40(5):431-447.

[22]   Jiang G, Gao J. Flow and heat transfer performance of the channel with different shaped ribs cooled by mist/steam two-phase flow. Case Stud Therm Eng. 2022;38:102365.

[23]   Eiamsa-ard S, Promvonge P. Thermal characteristics of turbulent rib-grooved channel flows. Int Commun Heat Mass Transf. 2009;36(7):705-711.

[24] Eiamsa-ard S, Promvonge P. Numerical study on heat transfer of turbulent channel flow over periodic grooves. Int Commun Heat Mass Transf. 2008;35(7):844–852.

[25] Eiamsa-ard S, Sripattanapipat S, Promvonge P. Influence of triangular wavy baffles on heat and fluid flow characteristics in a channel. J Mech Sci Tech. 2013;27:2199–2208.

[26] Wang L, Sundén B. Experimental investigation of local heat transfer in a square duct with various-shaped ribs. Heat Mass Transf. 2007;43:759–766.

[27] Xie G, Liu J, Ligrani PM, Sunden B. Flow structure and heat transfer in a square passage with offset mid-truncated ribs. Int J Heat Mass Transf. 2014;71:44–56.

[28] Iacovides H, Kelemenis G, Raisee M. Flow and heat transfer in straight cooling passages with inclined ribs on opposite walls: an experimental and computational study. Exp Therm Fluid Sci. 2003;27(3):283–294.

[29] Mahanand Y, Senapati JR. Thermo-hydraulic performance analysis of a solar air heater (SAH) with quarter-circular ribs on the absorber plate: A comparative study. Int J Therm Sci. 2021;161:106747.

[30] Ekiciler R, Çetinkaya MSA. A comparative heat transfer study between monotype and hybrid nanofluid in a duct with various shapes of ribs. Therm Sci Eng Progr. 2021;23:100913.

[31] Liu J, Hussain S, Wang J, Wang L, Xie G, Sunden B. Heat transfer enhancement and turbulent flow in a high aspect ratio channel (4:1) with ribs of various truncation types and arrangements. Int J Therm Sci. 2018;123:99–116.

[32] Liu J, Hussain S, Wang W, Xie G, Sunden B. Experimental and numerical investigations of heat transfer and fluid flow in a rectangular channel with perforated ribs. Int Commun Heat Mass. 2021;121:105083.

[33] Prasad BN, Saini JS. Effect of artificial roughness on heat transfer and friction factor in a solar air heater. Sol Energy. 1988;41(6):555–560.

[34] Prasad BN, Saini JS. Optimal thermohydraulic performance of artificial roughened solar air heater. Sol Energy. 1991;47(2):91–96.

[35] Eiamsa-ard S, Sripattanapipat S, Promvonge P. Simulation of turbulent channel flow over two blocks in tandem arrangement. Proceedings of the Tenth Asian Congress of Fluid Mechanics (ACFMX); 2004 May 17–21; Sri Lanka; 2004. p. C–17.

[36] Promvonge P, Changcharoen W, Kwankaomeng S, Thianpong C. Numerical heat transfer study of turbulent square-duct flow through inline V-shaped discrete ribs. Int Commun Heat Mass. 2011;38(10):1392–1399.

[37] Bahiraei M, Mazaheri N, Hosseini Y, Moayedi H. A two-phase simulation for analyzing thermohydraulic performance of Cu-water nanofluid within a square channel enhanced with 90° V-shaped ribs. Int Commun Heat Mass. 2019;145:118612.

[38] Layek A, Saini JS, Solanki SC. Effect of chamfering on heat transfer and friction characteristics of solar air heater having absorber plate roughened with compound turbulators. Renew Energ. 2009;34(5):1292–1298.

[39] Momin AME, Saini JS, Solanki SC. Heat transfer and friction in solar air heater duct with V-shaped rib roughness on absorber plate. Int J Heat Mass Tran. 2002;45(16):3383–3396.

[40] Saini SK, Saini RP. Development of correlations for Nusselt number and friction factor for solar air heater with roughened duct having arc-shaped wire as artificial roughness. Sol Energy. 2008;82(12):1118–1130.

[41] Karwa R, Solanki SC, Saini JS. Heat transfer coefficient and friction factor correlations for the transitional flow regime in rib-roughened rectangular ducts. Int J Heat Mass Tran. 1999;42(9):1597–1615.

[42]   Bhagoria JL, Saini JS, Solanki SC. Heat transfer coefficient and friction factor correlations for rectangular solar air heater duct having transverse wedge shaped rib roughness on the absorber plate. Renew Energ. 2002;25(3):341–369.

[43]   Jaurker AR, Saini JS, Gandhi BK. Heat transfer and friction characteristics of rectangular solar air heater duct using rib-grooved artificial roughness. Sol Energy. 2006;80(8):895–907.

[44]   Karmare SV, Tikekar AN. Heat transfer and friction factor correlation for artificially roughened duct with metal grit ribs. Int J Heat Mass Tran. 2007;50(21–22):4342–4351.

[45]   Saini RP, Verma J. Heat transfer and friction factor correlations for a duct having dimple-shape artificial roughness for solar air heaters. Energy. 2008;33(8):1277–1287.

[46]   Yadav AS, Bhagoria JL. A CFD (computational fluid dynamics) based heat transfer and fluid flow analysis of a solar air heater provided with circular transverse wire rib roughness on the absorber plate. Energy. 2013;55:1127–1142.

[47]   Yadav AS, Bhagoria JL. A numerical investigation of square sectioned transverse rib roughened solar air heater. Int J Therm Sci. 2014;79:111–131.

[48]   Yadav AS, Bhagoria JL. A CFD based thermo-hydraulic performance analysis of an artificially roughened solar air heater having equilateral triangular sectioned rib roughness on the absorber plate. Int J Heat Mass Tran. 2014;70:1016–1039.

[49]   Aharwal KR, Gandhi BK, Saini JS. Experimental investigation on heat-transfer enhancement due to a gap in an inclined continuous rib arrangement in a rectangular duct of solar air heater. Renew Energ. 2008;33(4):585–596.

[50]   Aharwal KR, Gandhi BK, Saini JS. Heat transfer and friction characteristics of solar air heater ducts having integral inclined discrete ribs on absorber plate. Int Commun Heat Mass. 2009;52(25–26):5970–5977.

[51]   Sahu MM, Bhagoria JL. Augmentation of heat transfer coefficient by using 90o broken transverse ribs on absorber plate of solar air heater. Renew Energ. 2005;30(13):2057–2073.

[52]   Varun, Saini RP, Singal SK. Investigation of thermal performance of solar air heater having roughness elements as a combination of inclined and transverse ribs on the absorber plate. Renew Energ. 2008;33(6):1398–1405.

[53]   Boonloi A, Jedsadaratanachai W. CFD analysis on heat transfer characteristics and fluid flow structure in a square duct with modified wavy baffles. Case Stud Therm Eng. 2022;29:101660.

[54]   Boonloi A, Jedsadaratanachai W. Numerical investigation on turbulent forced convection and heat transfer characteristic in a square channel with discrete combined V-baffle and V-orifice. Case Stud Therm Eng. 2016;8:226–235.

[55]   Chaube A, Gupta S, Verma P. Heat transfer and friction factor enhancement in a square channel having integral inclined discrete ribs on two opposite walls. J Mech Sci Technol. 2014;28:1927–1937.

[56]   Kaewchoothong N, Maliwan K, Takeishi K, Nuntadusit C. Effect of inclined ribs on heat transfer coefficient in stationary square channel. Theor Appl Mech Lett. 2007;7(6):344–350.

[57]   Han JC, Zhang YM, Lee CP. Augmented heat transfer in square channels with parallel, crossed and V-shaped angled ribs. J Heat Trans-T ASME. 1991;113(3):590–596.

[58]   Han JC, Zhang YM, Lee CP. Influence of surface heat flux ratio on heat transfer augmentation in square channels with parallel, crossed, and V-shaped angled ribs. J Turbomach. 1992;114(4):872–880.

[59]   Xie G, Zheng S, Zhang W, Sundén B. A numerical study of flow structure and heat transfer in a square channel with ribs combined downstream half-size or same-size ribs. Appl Therm Eng. 2013;61(2):289–300.

[60]   Kumar A, HoeKim M. Heat transfer and fluid flow characteristics in air duct with various V-pattern rib roughness on the heated plate: A comparative study. Energy. 2016;103:75–85.

[61]   Abraham S, Vedula RP. Heat transfer and pressure drop measurements in a square cross-section converging channel with V and W rib turbulators. Exp Therm Fluid Sci. 2016;70:208-219.

[62]   Han JC, Zhang YM. High performance heat transfer ducts with parallel broken and V-shaped broken ribs. Int J Heat Mass Tran. 1992;35(2):513-523.

[63]   Karwa R. Experimental studies of augmented heat transfer and friction in asymmetrically heated rectangular ducts with ribs on the heated wall in transverse, inclined, V-continuous and V discrete pattern. Int Commun Heat Mass. 2003;30(2):241-250.

[64]   Tanda G, Abram R. Forced convection heat transfer in channels with rib turbulators inclined at 45 deg. J Turbomach Trans ASME. 2009;131(2):021012.

[65]   Bazdid-Tehrani F, Naderi-Abadi M. Numerical analysis of laminar heat transfer in entrance region of a horizontal channel with transverse fins. Int Commun Heat Mass. 2004;31(2):211-220.

[66]   Mousavi SS, Hooman K. Heat and fluid flow in entrance region of a channel with staggered baffles. Energ Convers Manage. 2006;47(15-16):2011-2019.

[67]   Chang SW, Chen TW, Chen YW. Detailed heat transfer and friction factor measurements for square channel enhanced by plate insert with inclined baffles and perforated slots. Appl Therm Eng. 2019;159:113856.

[68]   Mashaei PR, Taheri-Ghazvini M, Moghadam RS, Madani S. Smart role of Al2O3-water suspension on laminar heat transfer in entrance region of a channel with transverse in-line baffles. Appl Therm Eng. 2017;112:450-463.

[69]   Promvonge P, Sripattanapipat S, Kwankaomeng S. Laminar periodic flow and heat transfer in square channel with 45° inline baffles on two opposite walls. Int J Therm Sci. 2010;49:963-975.

[70]   Promvonge P, Sripattanapipat S, Tamna S, Kwankaomeng S, Thianpong C. Numerical investigation of laminar heat transfer in a square channel with 45° inclined baffles. Int Commun Heat Mass. 2010;37(2):170-177.

[71]   Kwankaomeng S, Promvonge P. Numerical prediction on laminar heat transfer in square duct with 30° angled baffle on one wall. Int Commun Heat Mass. 2010;37(7):857-866.

[72]   Promvonge P, Jedsadaratanachai W, Kwankaomeng S. Numerical study of laminar flow and heat transfer in square channel with 30° inline angled baffle turbulators. Appl Therm Eng. 2010;30(11-12):1292-1303.

[73]   Dutta S, Dutta P, Jones RE, Khan JA. Heat transfer coefficient enhancement with perforated baffles. J Heat Transf. 1998;120(3):795-797.

[74]   Dutta P, Dutta S. Effect of baffle size, perforation, and orientation on internal heat transfer enhancement. Int J Heat Mass Tran. 1998;41:3005-3013.

[75]   Sahel D, Ameur H, Benzeguir R, Kamla Y. Enhancement of heat transfer in a rectangular channel with perforated baffles. Appl Therm Eng. 2016;101:156-164.

[76]   El Habet MA, Ahmed SA, Saleh MA. The effect of using staggered and partially tilted perforated baffles on heat transfer and flow characteristics in a rectangular channel. Int J Therm Sci. 2022;174:107422.

[77]   Alam T, Saini RP, Saini JS. Experimental investigation on heat transfer enhancement due to V-shaped perforated blocks in a rectangular duct of solar air heater. Energ Convers Manage. 2014;81:374-383.

[68]   Chamoli S. A Taguchi approach for optimization of flow and geometrical parameters in a rectangular channel roughened with V down perforated baffles. Case Stud Therm Eng. 2015;5:59-69.

[79] Chamoli S, Thakur NS. Heat transfer enhancement in solar air heater with V-shaped perforated baffles. J Renew Sustain Ener. 2013;5:023122.

[80] Chamoli S, Thakur NS. Correlations for solar air heater duct with V-shaped perforated baffles as roughness elements on absorber plate. Int J Sustain Energy. 2016;35:1-20.

[81] Promvonge P, Skullong S. Thermal characteristics in solar air duct with V-shaped flapped-baffles and chamfered-grooves. Int J Heat Mass Tran. 2021;172:121220.

[82] Eiamsa-ard S, Sripattanapipat S, Promvonge P. Numerical heat transfer analysis in turbulent channel flow over a side-by-side triangular prism pair. J Eng Thermophys. 2012;21(2):95-110.

[83] Thakur DS, Khan MK, Pathak M. Solar air heater with hyperbolic ribs: 3D simulation with experimental validation. Renew Energ. 2017;113:357-368.

[84] Li Y, Rao Y, Wang D, Zhang P, Wub X. Heat transfer and pressure loss of turbulent flow in channels with miniature structured ribs on one wall. Int J Heat Mass Tran. 2019;131:584-593.

[85] Jiang W, Zhao J, Rao Z. Heat transfer performance enhancement of liquid cold plate based on mini V-shaped rib for battery thermal management. Appl Therm Eng. 2021;189:116729.

[86] Tanda G, Satta F. Heat transfer and friction in a high aspect ratio rectangular channel with angled and intersecting ribs. Int J Heat Mass Tran. 2021;169:120906.

[87] Jin D, Zhang M, Wang P, Xu S. Numerical investigation of heat transfer and fluid flow in a solar air heater duct with multi V-shaped ribs on the absorber plate. Energy 2015;89:178-190.

[88] Jin D, Quan S, Zuo J, Xu S. Numerical investigation of heat transfer enhancement in a solar air heater roughened by multiple V-shaped ribs. Renew Energ. 2019;134:78-88.

[89] Li J-L, Tang HW, Yang Y-T. Numerical simulation and thermal performance optimization of turbulent flow in a channel with multi V-shaped baffles. Int Commun Heat Mass. 2018;92:39-50.

[90] Fawaz HE, Badawy MTS, Abd Rabbo MF, Elfeky A. Numerical investigation of fully developed periodic turbulent flow in a square channel fitted with 45° in-line V-baffle turbulators pointing upstream. Alex Eng J. 2018;57(2):633-642.

[91] Dong Z, Liu P, Xiao H, Liu Z, Liu W. A study on heat transfer enhancement for solar air heaters with ripple surface. Renew Energ. 2021;172:477-487.

[92] Singh AP, Varun, Siddhartha. Heat transfer and friction factor correlations for multiple arc shape roughness elements on the absorber plate used in solar air heaters. Exp Therm Fluid Sci. 2014;54:117-126.

[93] Singh S, Chande S, Saini JS. Investigations on thermo-hydraulic performance due to flow-attack-angle in V-down rib with gap in a rectangular duct of solar air heater. Appl Energ. 2012;97:907-912.

[94] Singh S, Chander S, Saini JS. Thermo-hydraulic performance due to relative roughness pitch in V-down rib with gap in solar air heater duct – Comparison with similar rib roughness geometries. Renew Sust Energ Rev. 2015;43:1159-1166.

[95] Kumar A, Saini RP, Saini JS. Development of correlations for Nusselt number and friction factor for solar air heater with roughened duct having multi v-shaped with gap rib as artificial roughness. Renew Energ. 2013;58:151-163.

[96] Maithani R, Saini JS. Heat transfer and friction factor correlations for a solar air heater duct roughened artificially with V-ribs with symmetrical gaps. Exp Therm Fluid Sci. 2016;70:220-227.

[97] Kumar R, Kumar A, Chauhan R, Sethi M. Heat transfer enhancement in solar air channel with broken multiple V-type baffle. Case Stud Therm Eng. 2016;8:187-197.

[98]   Jedsadaratanachai W, Boonloi A. Effects of blockage ratio and pitch ratio on thermal performance in a square channel with 30° double V-baffles. Case Stud Therm Eng. 2014;4:118-128.

[99]   Jedsadaratanachai W, Boonloi A. Numerical investigation on turbulent forced convection and heat transfer characteristic in a square channel with discrete combined V-baffle and V-orifice. Case Stud Therm Eng. 2016;8:226-235.

[100]   Kumar R, Chauhan R, Sethi M, Kumar A. Experimental study and correlation development for Nusselt number and friction factor for discretized broken V-pattern baffle solar air channel. Exp Therm Fluid Sci. 2017;81:56-75.

[101]   Kumar R, Sethi M, Chauhan R, Kumar A. Experimental study of enhancement of heat transfer and pressure drop in a solar air channel with discretized broken V-pattern baffle. Renew Energ. 2017;101:856-872.

[102]   Promvonge P, Skullong S. Augmented heat transfer in tubular heat exchanger fitted with V-baffled tapes. Int J Therm Sci. 2020;155:106429.

[103]   Promvonge P, Skullong S. Enhanced thermal performance in tubular heat exchanger contained with V-shaped baffles. Appl Therm Eng. 2021;185:116307.

[104]   Phila A, Thianpong C, Eiamsa-ard S. Influence of geometric parameters of alternate axis twisted baffles on the local heat transfer distribution and pressure drop in a rectangular channel using a transient liquid crystal technique. Energies. 2019;12(12):2341.

[105]   Eiamsa-ard S. Study on thermal and fluid flow characteristics in turbulent channel flows with multiple twisted tape vortex generators. Int Commun Heat Mass. 2010;37(6):644-651.

[106]   Kumar A, Layek A. Thermo-hydraulic performance of solar air heater having twisted rib over the absorber plate. Int J Therm Sci. 2018;133:181-195.

[107]   Kumar A, Layek A. Nusselt number and friction factor correlation of solar air heater having twisted-rib roughness on absorber plate. Renew Energ. 2019;130:687-699.

[108]   Rashidi S, Akbarzadeh M, Karimi N, Masoodi R. Combined effects of nanofluid and transverse twisted-baffles on the flow structures, heat transfer and irreversibilities inside a square duct – A numerical study. Appl Therm Eng. 2018;130:135-148.

[109]   Zhang Q, Feng Z, Li Z, Chen Z, Huang S, Zhang J, Guo F. Numerical investigation on hydraulic and thermal performances of a mini-channel heat sink with twisted ribs. Int J Therm Sci. 2022;179:107718.

[110]   Sawhney JS, Maithani R, Chamoli S. Experimental investigation of heat transfer and friction factor characteristics of solar air heater using wavy delta winglets. Appl Therm Eng. 2017;117:740-751.

[111]   Sahu MK, Prasad RK. Exergy based performance evaluation of solar air heater with arc- shaped wire roughened absorber plate. Renew Sust Energ Rev. 2016;96:233-243.

[112]   Hans VS, Gill RS, Singh S. Heat transfer and friction factor correlations for a solar air heater duct roughened artificially with broken arc ribs. Exp Therm Fluid Sci. 2017;80:77-89.

[113]   Saravanakumar PT, Somasundaram D, Matheswaran MM. Thermal and thermo-hydraulic analysis of arc shaped rib roughened solar air heater integrated with fins and baffles. Sol Energy. 2019;180:360-371.

[114]   Promvonge P, Eiamsaard S, Wongcharee K, Chuwattanakul V, Samruaisin P, Chokphoemphun S, Nanan K, Eiamsa-ard P. Characterization of heat transfer and artificial neural networks prediction on overall performance index of a channel installed with arc-shaped baffle turbulators. Case Stud Therm Eng. 2021;26:101067.

[115]   Sureandhar G, Srinivasan G, Muthukumar P, Senthilmurugan S. Investigation of thermal performance in a solar air heater having variable arc ribbed fin configuration. Sustain Energy Technol Assess. 2022;52:102069.

[116] Promvonge P, Chompookham T, Kwankaomeng S, Thianpong C. Enhanced heat transfer in a triangular ribbed channel with longitudinal vortex generators. Energy Convers Manag. 2010;51(6):1242–1249.

[117] Promvonge P, Khanoknaiyakarn C, Kwankaomeng S, Thianpong C. Thermal behavior in solar air heater channel fitted with combined rib and delta-winglet. Int Commun Heat Mass. 2011;38(6):749–756.

[118] Nazir U, Sohail M, Hafeez MB, Krawczuk M, Askar S, Wasif S. An inclination in thermal energy using nanoparticles with casson liquid past an expanding porous surface. Energies. 2021;14(21):7328.

[119] Ahmed Z, Saleem S, Nadeem S, Khan AU. Squeezing flow of carbon nanotubes-based nanofluid in channel considering temperature-dependent viscosity: a numerical approach. Arab J Sci Eng. 2021;46:2047–2053.

[120] Saleem S, Gopal D, Shah NA, Feroz N, Kishan N, Chung JD, Safdar S. Modelling entropy in magnetized flow of eyring–powell nanofluid through nonlinear stretching surface with chemical reaction: a finite element method approach. Nanomaterials. 2022;12(11):1811.

Notes on contributors

Smith Eiamsa-ard is a mechanical engineering professor at Mahanakorn University of Technology (MUT). He was born in SakonNakhon province and studied high school at Sakolrajwittayanukul School in SakonNakhon. He continued his high school education at Maize high school in Wichita, Kansas, USA. He obtained a bachelor of engineering degree in mechanical engineering from MUT in 1996. He has been working at MUT since 1996. He has been working at MUT since 1996. He earned his M.Eng. and D.Eng. degrees in mechanical engineering from King Mongkut's Institute of Technology Ladkrabang (KMITL) and his Ph.D. degree in system engineering from Mie University, Japan, with a grant from MUT. He is mainly interested in thermal and fluid engineering, with a focus on heat transfer enhancement and computational fluid dynamics. He currently researches utilising swirling flow in various applications such as heat exchangers, solar air heaters, vortex tubes, and vortex combustors.

Arnut Phila received the D.Eng. in Mechanical Engineering from King Mongkut's Institute of Technology Ladkrabang (KMITL), in 2018. He has been working at Mahanakorn University of Technology (MUT) since 2006. Currently, he is an Assistant Professor of Mechanical Engineering at Mahanakorn University of Technology, Thailand. His research interests include energy technology and management, drying technology, industrial ovens and furnaces, and heat transfer enhancement.

Khwanchit Wongcharee is an Assistant Professor of chemical engineering at Mahanakorn University of Technology, Thailand. She received her Ph.D. in Chemical Engineering from University of New South Wales. Her research focuses on heat transfer enhancement and renewable energy.

Naoki Maruyama is a Professor of Regional Innovation Studies at Mie University, Japan. He holds BS and MS degrees in Mechanical Engineering from Mie University in 1986 and 1988, respectively, and become a Doctor of Engineering at Nagoya University, Japan in 1998. His current research interests include heat and flow visualization, two-phase flow, energy conversion, environmental engineering and life cycle assessment.

Masafumi Hirota is a Professor of Department of Mechanical Engineering at Aichi Institute of Technology, Japan. He received his D.Eng. in Mechanical Engineering from Nagoya University in 1990, then worked as a Research Associate, Assistant Professor and Associate Professor at Nagoya University, and as a Professor at Mie University, Japan. His research interests include heat exchangers, air conditioning, heat pumps and multi-phase flow. His current work is focused on gas-liquid flow in multi pass channels, application of airflows in zone air-conditioning and freezing in gas-liquid flow in microchannels.